Frog Hopper

"Utility by Land and Sea"

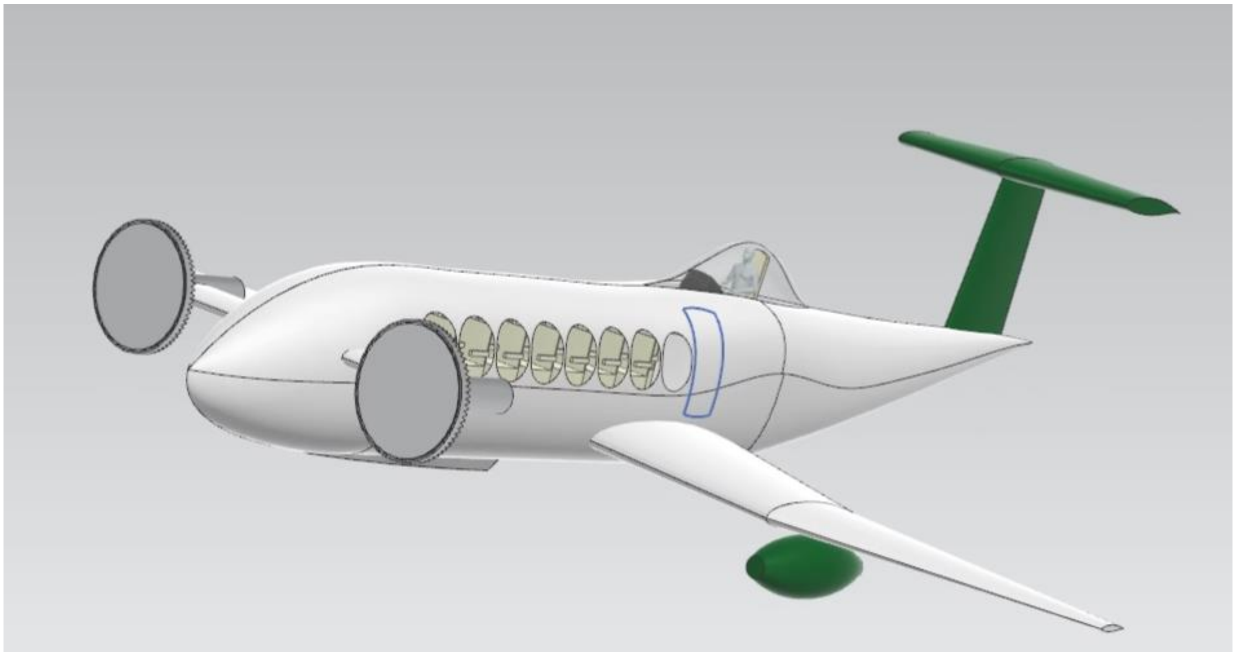

Riley Schwartzhoff

AIAA: 1421505

Riley Schwartzhoff

Advisor: Dr. Ronald Barrett-Gonzalez

AIAA: 022393

THE UNIVERSITY OF KANSAS

Acknowledgements

I would like to thank my parents Drew and Sara for their continued support throughout this process. I would also like to give thanks to Dr. Barrett for all of his extended guidance throughout this project.

Table of Contents Page #

Acknowledgements ii

List of Symbols iv

List of Acronyms v

Compliance Matrix vi

1 Introduction, General Concept of Operations, Mission Specification and Profile 1

2 Historical Review, Competition in the Market 4

2.1 Historical Review 4

2.2 Market Competition 7

3 Objectives, Requirements, and Design Optimization Function 9

3.1 Requirements 9

3.2 Objectives 11

3.3 Ancillary Objectives 11

3.4 Objective Function 12

3.5 Objective Flowdown Requirements 13

4 Statistical Time and Market Predicted Engineering Design (STAMPED) Analysis 15

4.1 We/Wto STAMPED Projection 15

4.2 L/D STAMPED Projection 16

5 Candidate Configuration Matrix Establishment 17

6 Application of Optimization Function and Requirements Flowdown Charts to Configurations and Downselection 17

7 Class I Weight Sizing 19

8 Class I Wing and Powerplant Sizing 20

9 Advanced Technologies and Design Concepts 23

9.1 Heilmeier's Catechism for Advanced Technology for Detachable Wings 23
10 V-n Diagram 25
11 Class I Cockpit and Fuselage Sizing 26
12 Class I Engine Installation 29
13 Class I Wing Layout Design 31
14 Class I Flight Control Device Sizing 33
15 Class I Empennage Sizing 33
16 Class I Landing Gear Sizing 35
17 Class II Landing Gear Sizing 36
18 Amphibious Characteristics 42
19 Aircraft Three-View and List of Salient Characteristics 44
20 Class II Weight and Balance 48
21 Class I Stability and Control 51
22 Class II Stability and Control 53
23 Class II Systems 54
23.1 Flight Control System 54
23.2 Fuel System 55
23.3 Hydraulic System 57
23.4 Electrical System 57
23.5 Environmental Control System 58
23.6 Cockpit Instrumentation 58
23.7 Anti-Icing System 59
23.8 Window Rain, Fog, and Frost Control System 60
24 Class I Structural Layout 60
25 Fault Tree Analysis 62
26 Ground Operations 65
27 Performance 69

28 Cost Analysis ... 70

29 Situational Renderings ... 72

30 References ... 74

List of Symbols

Symbols	**Description**	**Units**
A_{TOL}	Maximum Takeoff and Landing Altitude	ft (m)
AO_n	Ancillary Objective	(~)
$L_{STOL,dry}$	Dry Takeoff and Landing Length	ft (m)
$L_{STOL,wet}$	Wet Takeoff and Landing Length	ft (m)
O_n	Objective	(~)
OF_n	Objective Function	(~)
R_{1c}	Cargo Mission Requirement	(~)
R_{1p}	Passenger Mission Requirement	(~)
T_{rl}	Time to Reload	min
v_{cr}	Cruise Speed	kts ($\frac{km}{hr}$)
V_B	Baggage Volume	$\frac{ft^3}{passenger}$ ($\frac{m^3}{passenger}$)
W_B	Baggage Weight	$\frac{lb}{passenger}$ ($\frac{kg}{passenger}$)
W_e	Empty Weight	lb (kg)
W_P	Passenger Weight	$\frac{lb}{passenger}$ ($\frac{kg}{passenger}$)
W_{pl}	Payload Weight	lb (kg)
W_{to}	Takeoff Weight	lb (kg)

List of Acronyms

Acronyms	Description	Units
ADA	Americans with Disabilities Act	(~)
AIAA	American Institute of Aeronautics and Astronautics	(~)
CFR	Code of Federal Regulations	(~)
CONOPS	Concept of Operations	(~)
FAA	Federal Aviation Administration	(~)
FOD	Foreign Object Damage	(~)
FS	Fuselage Station	(~)
LIDAR	Light Detection and Range	(~)
NEWT	New Efficient Water and Terrestrial	(~)
RDT&E	Research, Development, Technology, and Engineering	(~)
RFP	Request for Proposal	(~)
STAMPED	Statistical Time and Market Predictive Engineering Design	(~)
STOL	Short Takeoff and Landing	(~)
VHF	Very High Frequency	(~)
WIG	Wing-In-Ground Effect	(~)

Compliance Matrix

RFP Objective	Demonstrated	Page No.
$\geq 200\ kts\ v_{cr}$	$v_{cr} = 250\ kts$	20
$\geq 19\ Passengers$	19 Passengers	27
$\geq 28\ in\ Seat\ Pitch$	30” of Pitch	27
$\geq 250\ nmi\ Range$ Passenger Mission	511 nmi Breguet Range	69
$\geq 193.6\ \frac{lb}{passenger}\ W_P$	$193.6\ \frac{lb}{passenger}$	19
$\geq 37.4\ \frac{lb}{passenger}\ W_B$	$37.4\ \frac{lb}{passenger}$	19
$\geq 4\ \frac{ft^3}{passenger} V_B$	$4\ \frac{ft^3}{passenger}$	66
$\leq 1500\ ft\ L_{STOL,dry}$	$1500\ ft\ L_{STOL,dry}$	20
$\leq 1900\ ft\ L_{STOL,wet}$	$1900\ ft\ L_{STOL,wet}$	20
$\geq 5000\ ft\ MSL\ A_{TOL}$	$5000\ ft\ MSL\ A_{TOL}$	20
$\geq 200\ nmi\ Range$ Cargo Mission	511 nmi Breguet Range	69
$\geq 5000\ lb\ W_{pl}$	$5000\ lb\ W_{pl}$	19
$\leq 60\ min\ T_{rl}$	$20\ min\ T_{rl}$	65

Design Philosophy: "To design a 19-passenger amphibious aircraft that offers versatility through interoperability as a wing-in-ground effect vehicle and provides a decrease in life cycle costs."

1 Introduction, General Concept of Operations, Mission Specification and Profile

In this section the concept of operations, mission specifications, and mission profiles were generated for the American Institute of Aeronautics and Astronautics (AIAA) New Efficient Water and Terrestrial (NEWT) aircraft request for proposal (RFP) [1]. There are a few major motivations of this design. One motivation is to create further connections between remote communities. This can improve the trade of supplies as well as allow for people to reach more remote areas more quickly. Another motivation is that this NEWT aircraft could also be utilized in

Figure 1.1: Frog Hopper Aircraft CONOPS

shuttling commuters in major cities where the airport is not near the city center. The potential versatility of the aircraft is a major part of the motivation. The concept of operations (CONOPS) of the aircraft can be seen in Figure 1.1 [2].

This CONOPS demonstrates the systems working together on the aircraft. The mission specification for the Frog Hopper can be seen in Table 1.1 below. This organizes the necessary requirements of the aircraft in a tabular format.

Table 1.1: NEWT Aircraft Mission Specification [3]

General Requirements	
Entry Into Service	2031 (Passenger Model)
Certification	FAA 14 CFR Part 23
Minimum Cruise Speed	200 knots (Target: 250 knots)
Flight Crew	1 pilot
Design Passenger Mission	
Passenger Capacity	19 people
Seat Pitch	Minimum 28”
Passenger Weight	193.6 lb
Baggage Weight/Volume	37.4 lb/4 ft^3 (per passenger)
Takeoff and Landing Situations	Dry pavement runway with 50’ obstacle at sea level; Dry pavement runway at 5,000 feet above mean sea level; Dirt, grass, metal mat, gravel, and asphalt at sea level; Water at sea level with 50’ obstacle; Water at 5,000 feet above mean sea level (replicates mountain lakes)
Maximum Dry/Water Take Off Distance	1,500’/1,900’
Range	250 nmi
Water Conditions	Sea State 3 Conditions
Design Cargo Mission	
Payload	5000 lb

Takeoff and Landing Situations	Dry pavement runway with 50’ obstacle at sea level; Water at sea level
Mission Turn Over Requirements	Can unload, refuel, and reload cargo in under 60 minutes
Range	200 nmi
Economic Mission	
Passenger and Baggage Loads	Same as for passenger mission
Range	150 nmi
Mission Characteristics	Optimized for minimum energy cost

While the mission specification gives important design requirements for the aircraft, mission profiles can visualize an aircraft’s mission effectively. Mission profiles for the passenger mission and the cargo mission can be seen in Figure 1.2 and Figure 1.3.

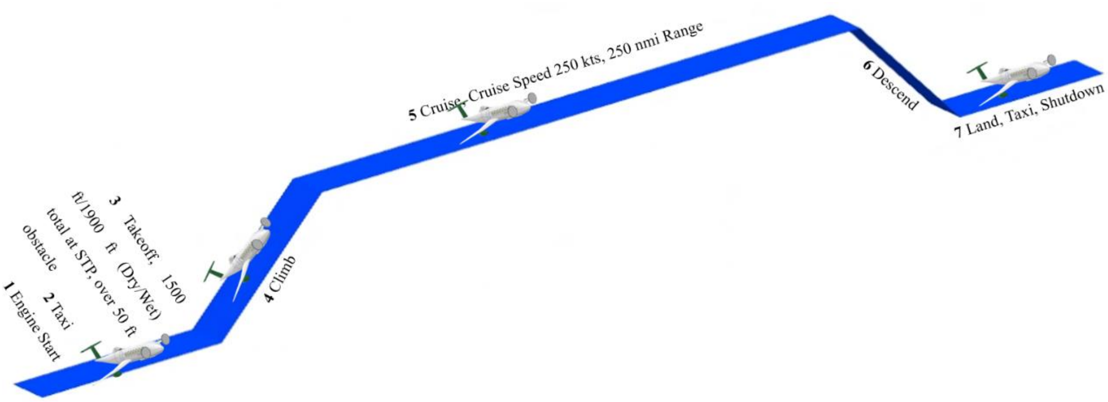

Figure 1.2: Passenger Mission Profile

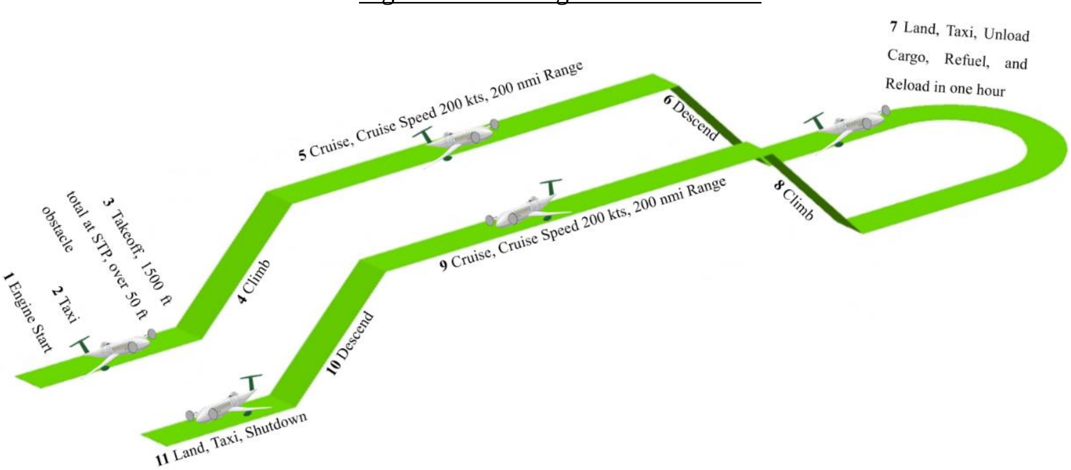

Figure 1.3: Cargo Mission Profile

The above mission profiles demonstrate the different takeoff requirements depending on which surface is being taken off from as well as the major differences between the passenger and cargo missions.

2 Historical Review, Competition in the Market

This section will examine existing aircraft similar to what is discussed in the mission specification as well as which of these aircraft are most successful in the market. 19 passenger commuters are the type of aircraft that are being investigated.

2.1 Historical Review

The Beechcraft 1900 was developed from the Super King Air line of aircraft in the late 1970s. This lineage of aircraft began in 1949 with the five-seat Beechcraft Model 50 Twin Bonanza. Several iterations of lengthening and enlarging this original frame led to production of the 19-passenger 1900 in 1982. Shortly after the 1900 was introduced, the Beechcraft 1900C was developed. The 1900C eliminated the aft passenger door of the 1900 and added a large cargo door. Additionally, the portions of the wings were used for fuel. Several years later a substantial redesign was done, leading to the Beechcraft 1900D being introduced in 1991. This model introduced a “stand-up cabin” which allows most passengers to walk upright in the aisle. This aircraft is only land-based. The Beechcraft 1900 series of aircraft stopped being produced in 2002, but many are still in service today [4], [5].

Figure 2.1.1: Beechcraft 1900D [5]

The British Aerospace Jetstream 31 is a 19-passenger aircraft that had its development start in 1978. The Jetstream 31 was developed from the Handley Page Jetstream, after Scottish Aviation took over production from Handley Page before being nationalized with other aerospace manufacturers into British Aerospace. The Jetstream 31 had its first flight in 1980, before starting production in 1982. This aircraft is only land-based. Production was shut down in 1993 but the aircraft remains in service today [4], [6].

Figure 2.1.2: British Aerospace Jetstream 31 [4]

The De Havilland Canada DHC-6 Twin Otter began development in 1964. The aircraft was developed as a larger, twin engine replacement for the DHC-3 Otter. In addition to the size upgrade, the DHC-6 has design features that boost the short takeoff and landing (STOL) performance. First flight for the DHC-6 occurred in 1965, and production began in the same year. Aerodynamic and payload improvements were made in 1968 when Series 200 production began, and again in 1969 for Series 300 production. Production ended temporarily in 1988 until the production rights for the DHC-6 were acquired by Viking Air in 2006. This led to the development of Series 400 which significantly upgraded the avionics of the aircraft and introduced composites into the frame. This aircraft can take off and land on both land and water. Production for this series began in 2008 and are ongoing [4], [7], [8].

Figure 2.1.3: De Havilland Canada DHC-6 Twin Otter [7]

Dornier developed a new type of wing which was subsidized by the German government in the 1970s. This wing was used with a modified Do 28D-2 Skyservant to develop the Dornier 128 aircraft. Development for an improved version of this aircraft, with a new fuselage, began in 1981. This became the 19-passenger Dornier 228. The Dornier 228 entered production in 1984 and is still being produced today. This aircraft is only land-based. The company which produced the aircraft has changed several times, but there has never been a period of stopped production [4], [8], [9].

Figure 2.1.4: Dornier 228 [4]

Harbin began a development of the Y-11 airframe that was named the Y-11T. Improvements from this design include a redesigned wing with a low drag section as well as a larger fuselage that is bonded rather than being a riveted construction. Additionally, piston engines were replaced with turboprops. The Y-11T became known as the Y-12 and had its first flight in 1982 and started production the same year. This aircraft is only land based. Production is ongoing [8], [10].

Figure 2.1.5: Harbin Y-12 [10]

John Britten and Desmond Norman designed the Trislander as a development of the better-known Britten-Norman Islander. The motivation behind this decision was to give the aircraft a larger capacity. The Trislander stretched the fuselage, strengthened the landing gear, and added a third engine atop the fin

Figure 2.1.6: Britten-Norman Trislander [11]

on the centerline. First flight for the Trislander occurred in 1970. The Trislander is only land based. Production began in 1970 and went until 1983 [4], [11].

The Cessna 408 SkyCourier was launched in 2017 by Textron Aviation. At launch, an order for 50 aircraft was placed by FedEx. The SkyCourier is a high-wing, twin-turboprop design. First flight was originally scheduled for 2019, but this got pushed back to 2020. This aircraft is land based. Production began in 2021 and is ongoing [8], [12].

Figure 2.1.7: Cessna 408 SkyCourier [8]

In 1978, production of the Antonov An-78 transferred production to PZL Mielec in Poland. PZL Mielec then developed a westernized version of this aircraft which became the M28 Skytruck. The Skytruck utilizes a Pratt and Whitney turboprop engine with a five-blade propeller. First flight occurred in 1993, but it was not certified under FAR Part 23 until 2004. The PZL M28 Skytruck is a land-based aircraft. Production began in 1994 and is ongoing [8], [13].

Figure 2.1.8: PZL M28 Skytruck [13]

Design for the initial version of the Dornier Seastar began in 1982. This design was an amphibian aircraft with metal wings. Several changes were made for the second version of this aircraft. The largest one of these changes was the transition to composite wings. Additionally, the hull bottom was flattened, the cockpit enlarged, and the nose reprofiled. The wing struts were also removed. This version was named the Dornier Seastar CD2. The CD2 had its first flight in 1987. This aircraft can operate from land and sea, and completed its seaworthiness trials in the Baltic Sea. The CD2 was FAA certified in 1991, but production didn’t actually begin until 2008 and is ongoing [8], [14].

Figure 2.1.9: Dornier Seastar CD2 [14]

Figure 2.1.10: Canadair CL-415 [15]

The Canadair CL-215 was the first aircraft designed specifically for usage as a water bomber. The aircraft was introduced in 1966, and a total of 125 aircraft were manufactured. The success of this aircraft led to the development of the slightly smaller, Canadair CL-415. The CL-415 was designed largely for the purpose of aerial firefighting, but it also has seen use in search and rescue operations. Both the CL-215 and CL-415 are amphibious aircraft. The CL-415 had its first flight in 1993 and began production in 1994. Production is ongoing, even though it has changed companies between Canadair, Bombardier, Viking Air, and De Havilland Canada [4], [15].

2.2 Market Competition

This section will discuss how existing 19-passenger commuter aircraft have performed and are performing in the market. This will inform which characteristics are more popular among consumers, and in which direction the market is heading.

2.2.1 The 19 Passenger/Commuter Market

The Beechcraft 1900D has been out of production since 2002, so there isn't any information on recent trends. The last 10 years of the Beechcraft 1900D's production were still examined, when there were 345 aircraft produced to order [16]. A similar examination was done for the British Aerospace Jetstream 31, which showed that there were 408 aircraft produced for order between 1983 and 1993 [17].

The most recent production order data that could be found for the Dornier 228 were orders from 2011. It was found that between 2001 and 2011 there were 8 228s produced for order [18]. Even though orders were decreased for the aircraft during this period, there has been an increase in orders recently. Specific order data for more recent years could not be found however. Production data for the last decade of De Havilland Canada DHC-6s can show the more recent market. In the last decade, there have been 121 Twin Otters produced [19].

2.2.2 Regional Aircraft Payload-Range Data and Operating Expenses

The payload-range data for several of the mentioned aircraft was found. The De Havilland Canada DHC-6 Twin Otter, Dornier Do 228, Beechcraft 1900D, and British Aerospace Jetstream 31 all have their payload range data plotted on below. This data can be used to find the correlating lift to drag ratios for the aircraft.

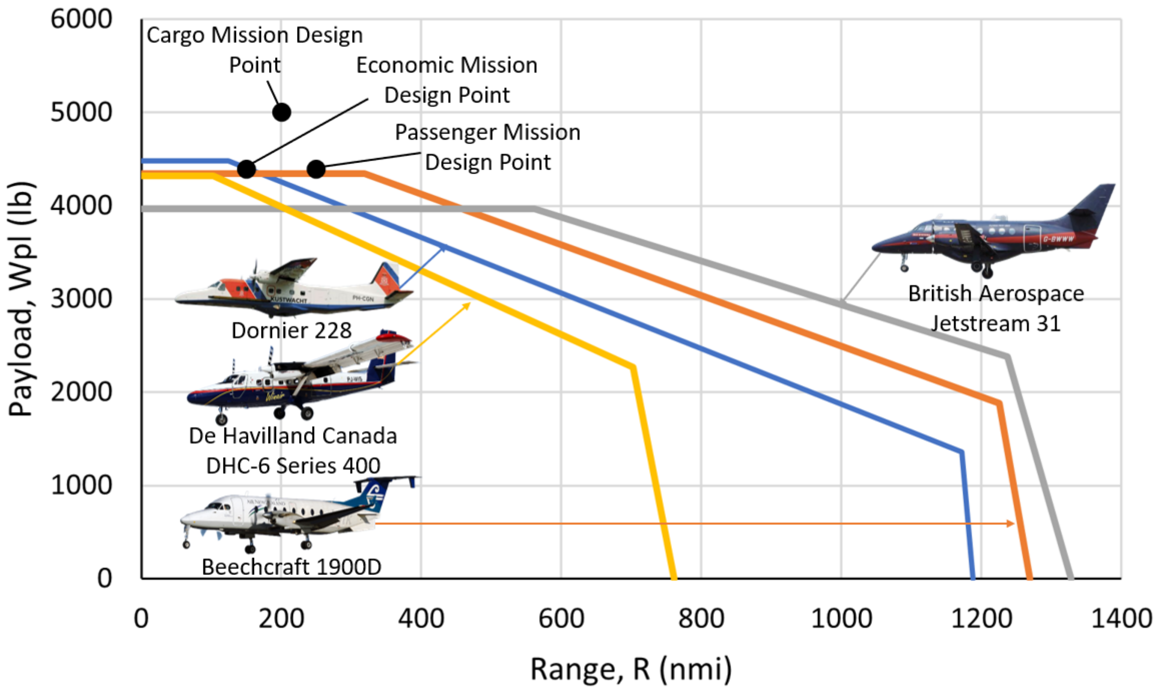

Figure 2.2.1: Dornier 228 Payload-Range Data [20]

2.2.3 19 Passenger Regional Aircraft Fleet Operating Norms

19-passenger aircraft are commonly used in regional airliner fleets. There isn't significant overlap in operating airlines between the aircraft that have been examined. The major operators of the Beechcraft 1900 are Ameriflight, Alpine Air Express, Searca, Central Mountain Air, SonAir, Air Georgian, SkyLink Express, Solenta Aviation, Exploits Valley Air Services, Twin Jet, Tropic Air, Pacific Coastal Airlines, Alaska Central Express, Propair Inc, Guna Airlines, Southern Airlines (Australia), and Trans Guyana Airways [5]. The British Aerospace Jetstream 31's major regional airlines are Northwestern Air, Pascan Aviation, SARPA, AIS Airlines, Transmandu, and FlyPelican [6]. The main operators of the De Havilland Canada DHC-6 are Trans Maldivian Airways, Grand Canyon Airlines, Kenn Borek Air, Maldivian, SonAir, Air Borealis, Air Inuit, Air Tindi, SVG Air, Zimex Aviation, Manta Air, Air Adelphi, Aviastar Mandiri, MASwings, LADE, and Seabird Airlines [7]. Lastly, the Dornier 228's major operators are Daily Air, Dornier Aviation Nigeria, New Central Airlines, Sevenair, and Summit air.

3 Objectives, Requirements, and Design Optimization Function

Objective functions are a way to mathematically score an aircraft design, showing how well the RFP is met. Requirements are specifications that must be met for the design to be approved. Objectives are specifications that are not mandatory to be met, but if met they help the strength of the design. Ancillary objectives are objectives not stated in the RFP that the designer comes up with. These can help a design stand out when compared to other responses to the RFP. The requirements, objectives, and ancillary objectives are then all combined into the objective function.

3.1 Requirements

Requirements for both the passenger mission and the cargo mission have to be considered. These requirements include minimum cruise speed (v_{cr}), passenger weight (W_P), baggage weight (W_B), baggage volume (V_B), dry takeoff and landing length ($L_{STOL,dry}$), water takeoff and landing length ($L_{STOL,wet}$), maximum takeoff and landing altitude (A_{TOL}) above mean sea level (MSL), time to reload (T_{rl}), and payload weight (W_{pl}). The requirements for the passenger mission and cargo mission can be seen in Table 3.1.1, Table 3.1.2, and Table 3.1.3 below.

Table 3.1.1: Frog Hopper Passenger Mission Requirements [15]

Requirement Number	Requirement	Values
R_{1p}	$\geq 200\ kts\ v_{cr}$	$\begin{cases} 1\ if\ v_{cr} \geq 200\ kts \\ 0\ if\ v_{cr} < 200\ kts \end{cases}$
R_{2p}	$\geq 1\ Flight\ Crew$	$\begin{cases} 1\ if\ Flight\ Crew \geq 1\ Person \\ 0\ if\ Flight\ Crew < 1\ Person \end{cases}$
R_{3p}	$\geq 19\ Passengers$	$\begin{cases} 1\ if\ Passengers \geq 19\ People \\ 0\ if\ Passengers < 19\ People \end{cases}$
R_{4p}	$\geq 28\ in\ Seat\ Pitch$	$\begin{cases} 1\ if\ Pitch \geq 28\ in \\ 0\ if\ Pitch < 28\ in \end{cases}$
R_{5p}	$\geq 250\ nmi\ Range$	$\begin{cases} 1\ if\ Range \geq 250\ nmi \\ 0\ if\ Range < 250\ nmi \end{cases}$
R_{6p}	$\geq 193.6\ \frac{lb}{passenger}\ W_P$	$\begin{cases} 1\ if\ W_P \geq 193.6\ \frac{lb}{passenger} \\ 0\ if\ W_P < 193.6\ \frac{lb}{passenger} \end{cases}$

Table 3.1.2: Frog Hopper Passenger Mission Requirements Continued [15]

Requirement Number	Requirement	Values
R_{7p}	$\geq 37.4\ \frac{lb}{passenger}\ W_B$	$\begin{cases} 1\ if\ W_B \geq 37.4\ \frac{lb}{passenger} \\ 0\ if\ W_B < 37.4\ \frac{lb}{passenger} \end{cases}$
R_{8p}	$\geq 4\ \frac{ft^3}{passenger} V_B$	$\begin{cases} 1\ if\ V_B \geq 4 \frac{ft^3}{passenger} \\ 0\ if\ V_B < 4\ \frac{ft^3}{passenger} \end{cases}$
R_{9p}	$\leq 1500\ ft\ L_{STOL,dry}$	$\begin{cases} 1\ if\ L_{STOL,dry} \leq 1500\ ft \\ 0\ if\ L_{STOL,dry} > 1500\ ft \end{cases}$
R_{10p}	$\leq 1900\ ft\ L_{STOL,wet}$	$\begin{cases} 1\ if\ L_{STOL,wet} \leq 1900\ ft \\ 0\ if\ L_{STOL,wet} > 1900\ ft \end{cases}$
R_{11p}	$\geq 5000\ ft\ MSL\ A_{TOL}$	$\begin{cases} 1\ if\ A_{TOL} \geq 5000\ ft\ MSL \\ 0\ if\ A_{TOL} < 5000\ ft\ MSL \end{cases}$

Table 3.1.3: Frog Hopper Cargo Mission Requirements [15]

Requirement Number	Requirement	Values
R_{1c}	$\geq 200\ kts\ v_{cr}$	$\begin{cases} 1\ if\ v_{cr} \geq 200\ kts \\ 0\ if\ v_{cr} < 200\ kts \end{cases}$
R_{2c}	$\geq 1\ Flight\ Crew$	$\begin{cases} 1\ if\ Flight\ Crew \geq 1\ Person \\ 0\ if\ Flight\ Crew < 1\ Person \end{cases}$
R_{3c}	$\geq 200\ nmi\ Range$	$\begin{cases} 1\ if\ Range \geq 200\ nmi \\ 0\ if\ Range < 200\ nmi \end{cases}$
R_{4c}	$\geq 5000\ lb\ W_{pl}$	$\begin{cases} 1\ if\ W_{pl} \geq 5000\ lb \\ 0\ if\ W_{pl} < 5000\ lb \end{cases}$
R_{5c}	$\leq 60\ min\ T_{rl}$	$\begin{cases} 1\ if\ T_{rl} \leq 60\ min \\ 0\ if\ T_{rl} > 60\ min \end{cases}$

Additionally, there is an ancillary requirement not listed in the RFP. It is important to follow the Americans with Disabilities Act (ADA) not just because it is morally right, but also because it is the law. This ancillary requirement is represented in Table 3.1.4 below.

Table 3.1.4: Frog Hopper Ancillary Requirement

Ancillary Requirement #	Ancillary Requirement	Values
AR_1	Americans with Disabilities Act (ADA) Compliant	$\begin{cases} 1\ if\ Aircraft\ is\ ADA\ compliant \\ 0\ if\ Aircraft\ is\ not\ ADA\ compliant \end{cases}$

3.2 Objectives

There is just one objective given in the RFP. This objective applies for both the passenger mission and the cargo mission. Additionally, visual appeal will be considered as an objective as it is mentioned as an important factor in the RFP. These objectives can be seen in Table 3.2.1 below.

Table 3.2.1: Frog Hopper Objectives [15]

Objective Number	Objective	Values
O_1	$\geq 250\ kts\ v_{cr}$	$\begin{cases} \frac{v_{cr} - 200kts}{50kts}\ if 200\ kts < v_{cr} < 250\ kts \\ 1\ if\ v_{cr} \geq 250\ kts \end{cases}$
O_2	Visually Appealing	$\begin{cases} 1\ if\ \%Appealing = 100\% \\ \frac{\%Appealing}{100}\ if\ \%Appealing \leq 100\% \end{cases}$

3.3 Ancillary Objectives

Ancillary objectives were determined using the author's engineering judgement. Ancillary objectives considered include the turnaround time, sterilizing the cabin quickly, operating in and out of ground effect, dry disembarkation at the dock, and complying with the Americans with Disabilities Act along with Stage 5 noise requirements. These ancillary objectives will significantly improve the aircraft for both the operator as well as the passengers. The ancillary objectives created can be seen in Table 3.3.1 below.

Table 3.3.1: Frog Hopper Ancillary Objectives

Ancillary Objective Number	Ancillary Objective	Values
AO_1	$\leq 30\ min\ T_{rl}$	$\begin{cases} \frac{T_{rl} - 30min}{30min}\ if\ 60\ min > T_{rl} > 30\ min \\ 1\ if\ T_{rl} \leq 30\ min \end{cases}$
AO_2	Interoperability as a wing-in-ground effect (WIG) aircraft	$\begin{cases} 1\ if\ Aircraft\ is\ interoperable\ as\ a\ WIG \\ 0\ if\ Aircraft\ is\ not\ interoperable\ as\ a\ WIG \end{cases}$
AO_3	Dry embarkation/ disembarkation at dock	$\begin{cases} 1\ if\ Aircraft\ has\ dry\ disembarkation \\ 0\ if\ Aircraft\ does\ not\ have\ dry\ disembarkation \end{cases}$
AO_4	Better than Stage 5 noise requirement	$\begin{cases} 1\ if\ Stage\ 5\ noise\ requirement\ is\ met \\ 0\ if\ Stage\ 5\ noise\ requirement\ is\ not\ met \end{cases}$
AO_5	Rapid cabin sterilization	$\begin{cases} 1\ if\ cabin\ can\ be\ sterilized\ rapidly \\ 0\ if\ cabin\ can'tbe\ sterilized\ rapidly \end{cases}$

3.4 Objective Function

Objective functions were created for both the passenger and cargo missions due to the different set of requirements. A relative objective waiting factor of two was used for both objective functions. The objective function can be seen below:

$$OF = AR_1 \prod_{i=1}^{11} R_{ip} \prod_{i=1}^{5} R_{ic} \left(\frac{1}{2}\sum_{j=1}^{2} O_j + \frac{1}{5*2}(AO_1 + 3AO_2 + AO_3 + AO_4 + AO_5)\right)$$

Ancillary objective 2 was weighted more than the other ancillary objectives. This was done because interoperability as a WIG is viewed as more important to this design than the other ancillary objectives due to the versatility that would be provided.

3.5 Objective Flowdown Requirements

The objectives for this design can be further broken down using flowdown charts. Tier 0 of this chart is where the objective is, and tier 1 is where system performance requirements are. Flowdown charts for the objectives and ancillary objectives containing tier 0 and tier 1 can be seen below. Boxes outlined in red affect the configuration of the aircraft.

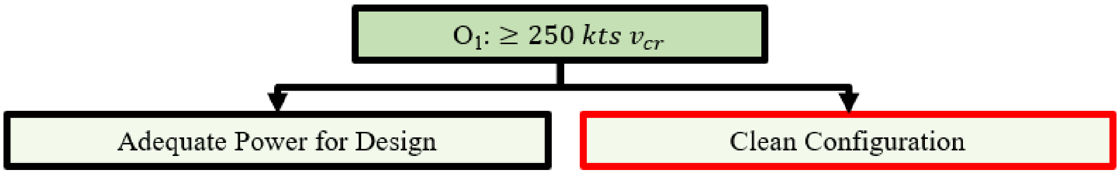

Figure 3.5.1: Objective 1 Flowdown Chart

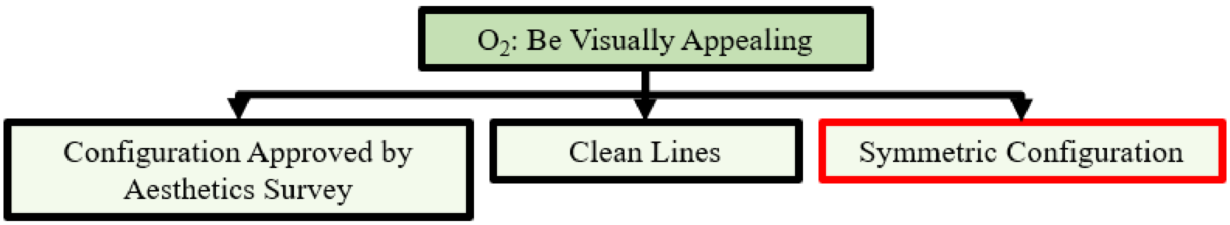

Figure 3.5.2: Objective 2 Flowdown Chart

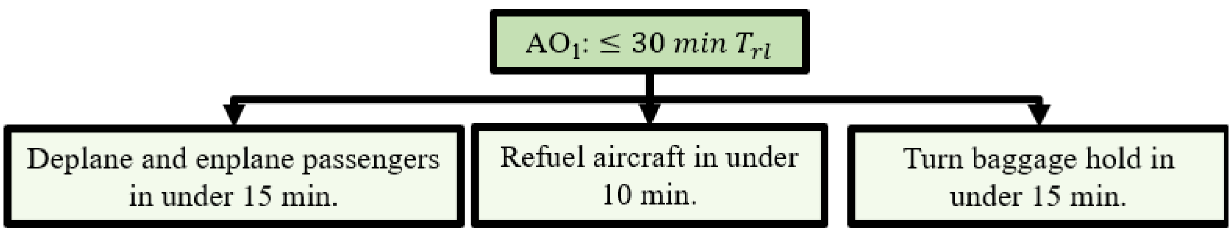

Figure 3.5.3: Ancillary Objective 1 Flowdown Chart

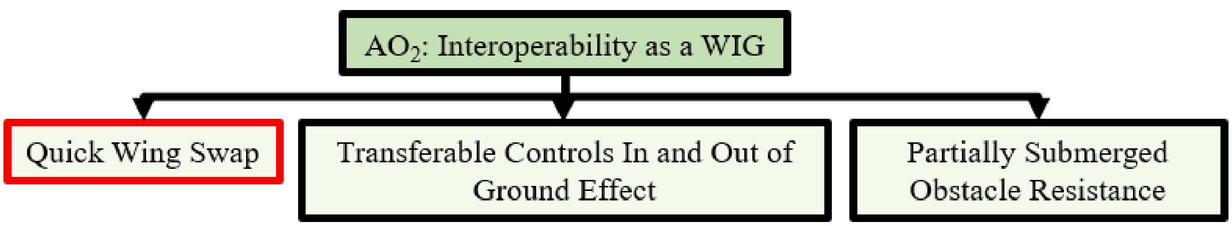

Figure 3.5.4: Ancillary Objective 2 Flowdown Chart

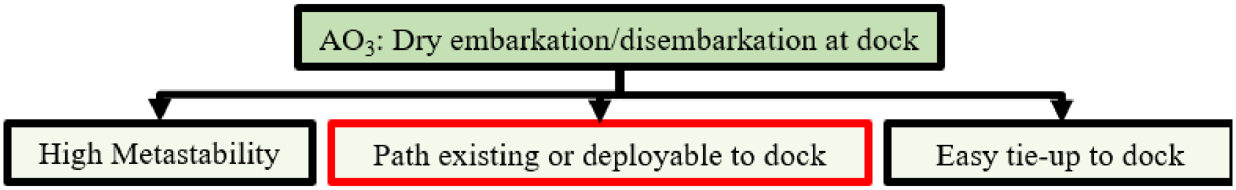

Figure 3.5.5: Ancillary Objective 3 Flowdown Chart

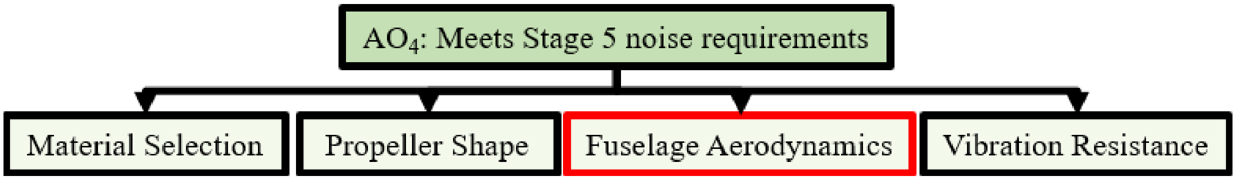

Figure 3.5.6: Ancillary Objective 4 Flowdown Chart

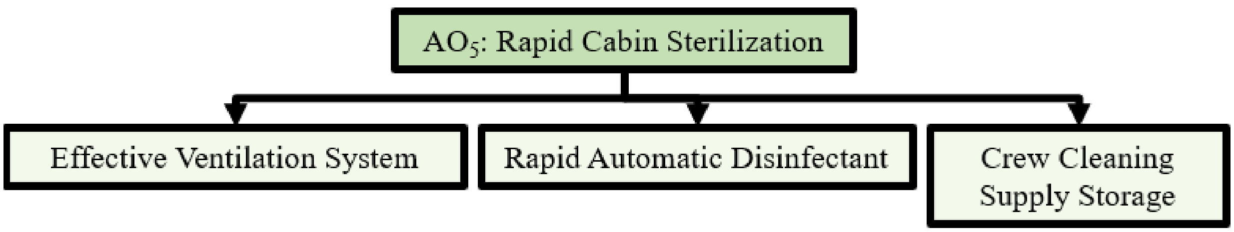

Figure 3.5.7: Ancillary Objective 5 Flowdown Chart

4 Statistical Time and Market Predicted Engineering Design (STAMPED) Analysis

In order to accurately predict how various design characteristics such as empty weight (W_e) to takeoff weight (W_{to}) ratio and the lift over drag ratio will trend into the future, a method of analysis known as Statistical Time and Market Predicted Engineering Design (STAMPED) analysis. This projection is necessary to undergo weight sizing for the aircraft. Both land-based and amphibious aircraft are considered.

4.1 W_e/W_{to} STAMPED Projection

The ratio of empty weight to takeoff weight for numerous land-based 19-passenger aircraft and amphibious 19-passenger aircraft were found and plotted. This was done to determine any trends that have arisen over time. Due

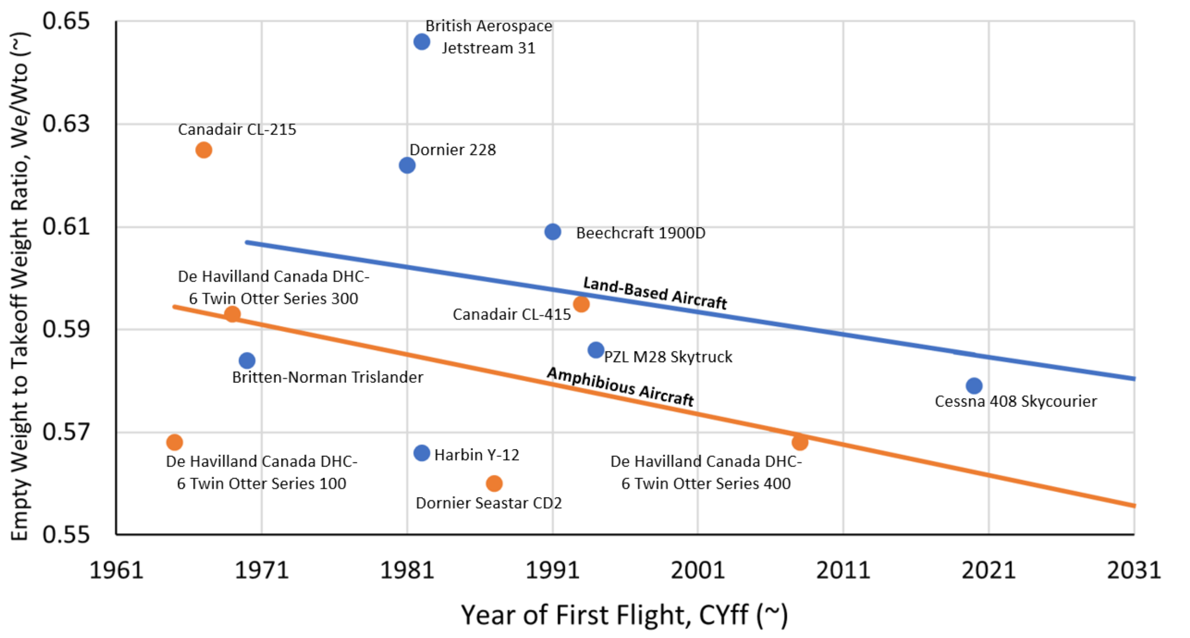

Figure 4.1.1: We/Wto STAMPED Data [4], [8], [10], [12], [14], [21], [22]

to the lack of amphibious aircraft with exactly 19 passengers, similarly sized aircraft were used. This data was then used to project these trends forward to the entry into service date of 2023. These trends can be seen in Figure 4.1.1.

The empty weight to takeoff weight ratio is decreasing with time for both the amphibious and land-based aircraft. Due to the intention to create an aircraft with interoperability as a WIG, the empty weight to takeoff weight ratio will increase. This leads to a more conservative ratio of 0.565 being selected.

4.2 L/D STAMPED Projection

L/D information was found for several of the aircraft using the Breguet range equation and the true mission fuel fraction. The payload-range data in Chapter 2.2.2 was utilized with these equations to calculate the lift to drag ratio. The calculation of the lift to drag ratio can be seen in Appendix A. These ratios were then projected to the entry into service date of 2031. This can be seen in Figure 4.2.1 below.

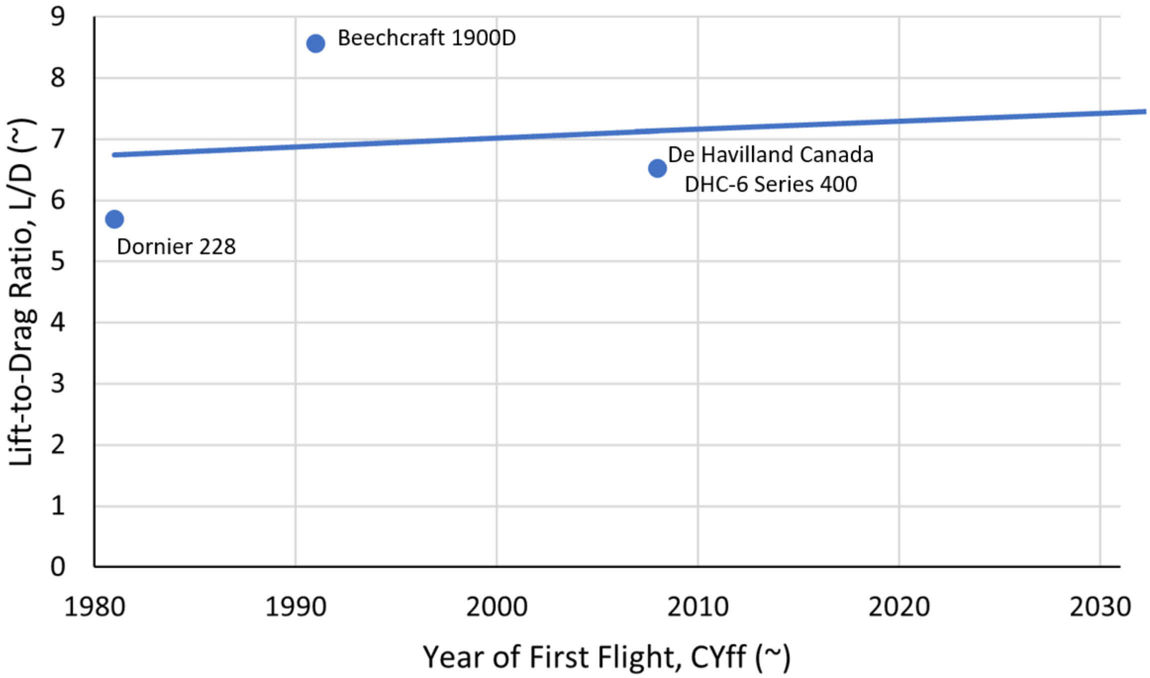

Figure 4.2.1: Lift to Drag Ratio STAMPED Data [4], [8], [23], [24]

This analysis results in a projected lift to drag ratio of 7.45 in 2031. This is a reasonable ratio to achieve, and the trend of the lift to drag ratio matches what was expected. This ratio of 7.45 is what will be used during the weight sizing process.

5 Candidate Configuration Matrix Establishment

The candidate configuration matrix is a collection of potential configurations for the aircraft. The matrix can be seen below.

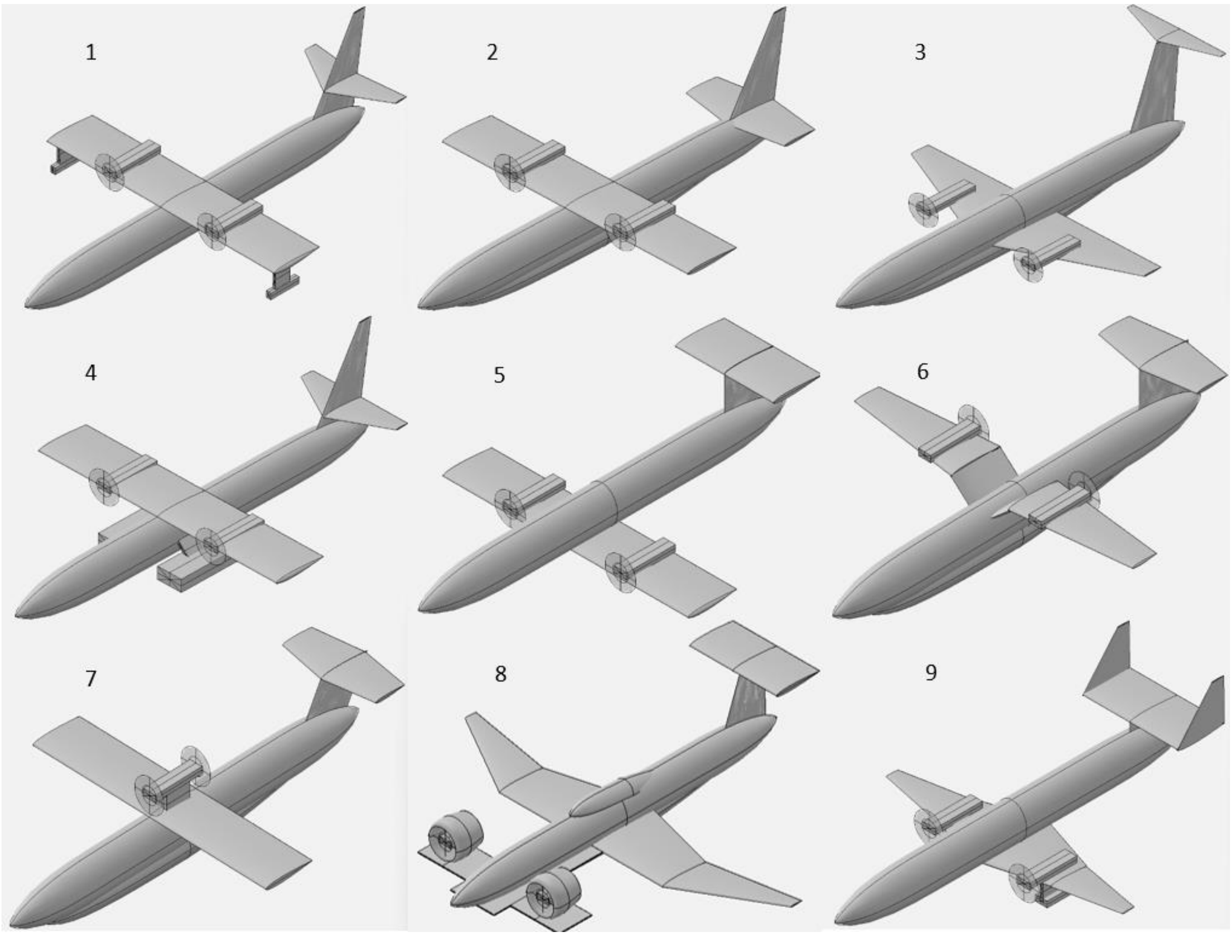

Figure 5.1: Candidate Configuration Matrix

6 Application of Optimization Function and Requirements Flowdown Charts to Configurations and Downselection

The optimization function and flowdown charts were used to downselect from the considered configurations to just one design that will be used in the sizing process. This is done to lessen the number of calculations that would need to be done if multiple configurations were carried through the weight sizing process. This downselection can be seen in Table 6.1 below.

Table 6.1: Configuration Downselection

	 Config 1	 Config 2	 Config 3	 Config 4	 Config 5	 Config 6	 Config 7	 Config 8	 Config 9
O1: v_cr≥ 250 kts	1	1	1	1	1	1	1	1	1
O2: Visually Appealing	0.7	0.8	1	0.9	0.6	0.5	0.2	0.4	0.3
Sum:	1.7	1.8	2	1.9	1.6	1.5	1.2	1.4	1.3
Weighted Sum:	0.85	0.9	0.9	0.9	0.8	0.75	0.6	0.7	0.65
AO1: ≤30 min T_rl	0.5	1	1	0.5	0.5	1	1	1	0.5
AO2: Interoperability as a WIG	0	0	0	0	0	0	0	1	0.75
AO3: Dry embarkation/ disembarkation at dock	0.6	0.8	0.8	0.6	1	0.5	0.8	0.6	1
AO4: Better than Stage 5 noise requirement	1	1	1	1	1	1	1	1	1
Cabin Sterilization	1	1	1	1	1	1	1	1	1
Sum:	3.1	3.8	3.8	3.1	3.5	3.5	3.8	6.6	5.75
Weighted Sum:	0.31	0.38	0.38	0.31	0.35	0.35	0.38	0.66	0.575
Total Score:	1.16	1.28	1.28	1.21	1.15	1.1	0.98	1.36	1.225

The downselection results in configuration 8 being selected to take through the sizing process. This configuration is inspired by the PESA report and takes a wing-in-ground effect design and adding extensions for full flight [25]. This will allow for the best interoperability as a WIG. Additionally, the luggage pod float allows for quick loading and unloading of cargo and would help protect against semi-submerged obstacles.

7 Class I Weight Sizing

Class I weight sizing was performed to determine an initial estimate of the takeoff weight of the aircraft. In order to achieve this, the process laid out in Jan Roskam's *Airplane Design Part I: Preliminary Sizing of Airplanes* was used. This process had to be followed for both the passenger mission and the cargo mission, as these two missions have different payload weights and ranges. The fuel fractions for these missions were found and can be seen in Table 7.1 below.

Table 7.1: Mission Weight Fractions

Weight Fraction	Segment	Passenger Mission	Cargo Mission
$\frac{W_1}{W_{TO}}$	Engine Start, Warm-up	0.992	0.992
$\frac{W_2}{W_1}$	Taxi	0.99	0.99
$\frac{W_3}{W_2}$	Take-off	0.996	0.996
$\frac{W_4}{W_3}$	Climb	0.985	0.985
$\frac{W_5}{W_4}$	Cruise	0.94	0.952
$\frac{W_6}{W_5}$	Descent	0.99	0.99
$\frac{W_7}{W_6}$	Landing, Taxi, Shutdown	0.99	0.99

These weight fractions were utilized to calculate the takeoff weight and the fuel weight of the aircraft in an iterative process. This process was iterated until the empty weight of the aircraft was within 0.5% of the guessed empty weight. Once this margin was achieved, the resulting weights can be seen in Table 7.2 below.

Table 7.2: Calculated Weights

Weight	Value (lb)
Empty Weight	8729
Takeoff Weight	15,500
Fuel Weight	1566

8 Class I Wing and Powerplant Sizing

Wing sizing was completed for takeoff, landing, climb, and cruise conditions. Both takeoff and landing calculations had to be performed for the case of being on land and on water, due to the amphibious characteristics of the Frog Hopper aircraft. The climb lines were calculated at half the intended cruise altitude of FL140. This verifies the ability to climb when taking off from 5000 ft ASL. The cruise altitude of FL140 was chosen as this altitude allows for the aircraft to be unpressurized, decreasing necessary cost and weight. This results in Figure 8.1 below.

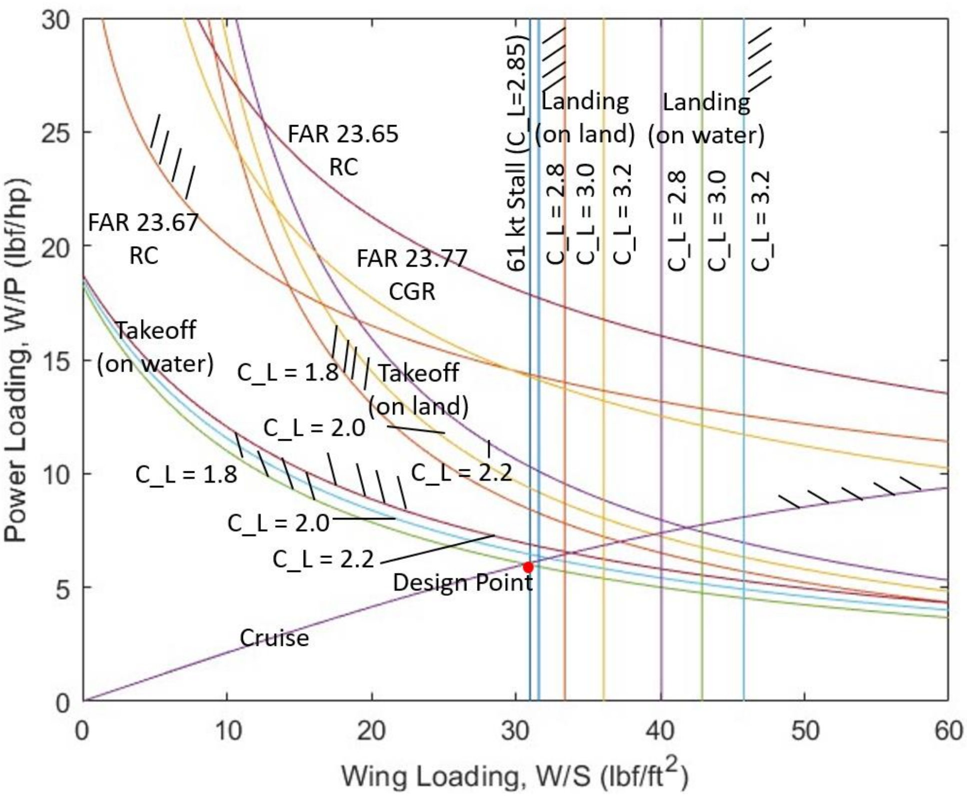

Figure 8.1: Class I Wing Sizing

A design point is selected at a wing loading of 30.7 $\frac{lb}{ft^2}$ and a power loading of 6.03 $\frac{lb}{hp}$. This allows for the wing area to be calculated to be 505 ft^2 and the power required to be calculated to be 2570 hp. This design point also ensures that the target cruise velocity of 250 kts is obtained. The drag polars for the aircraft were also calculated and can be seen in Figure 8.2 below.

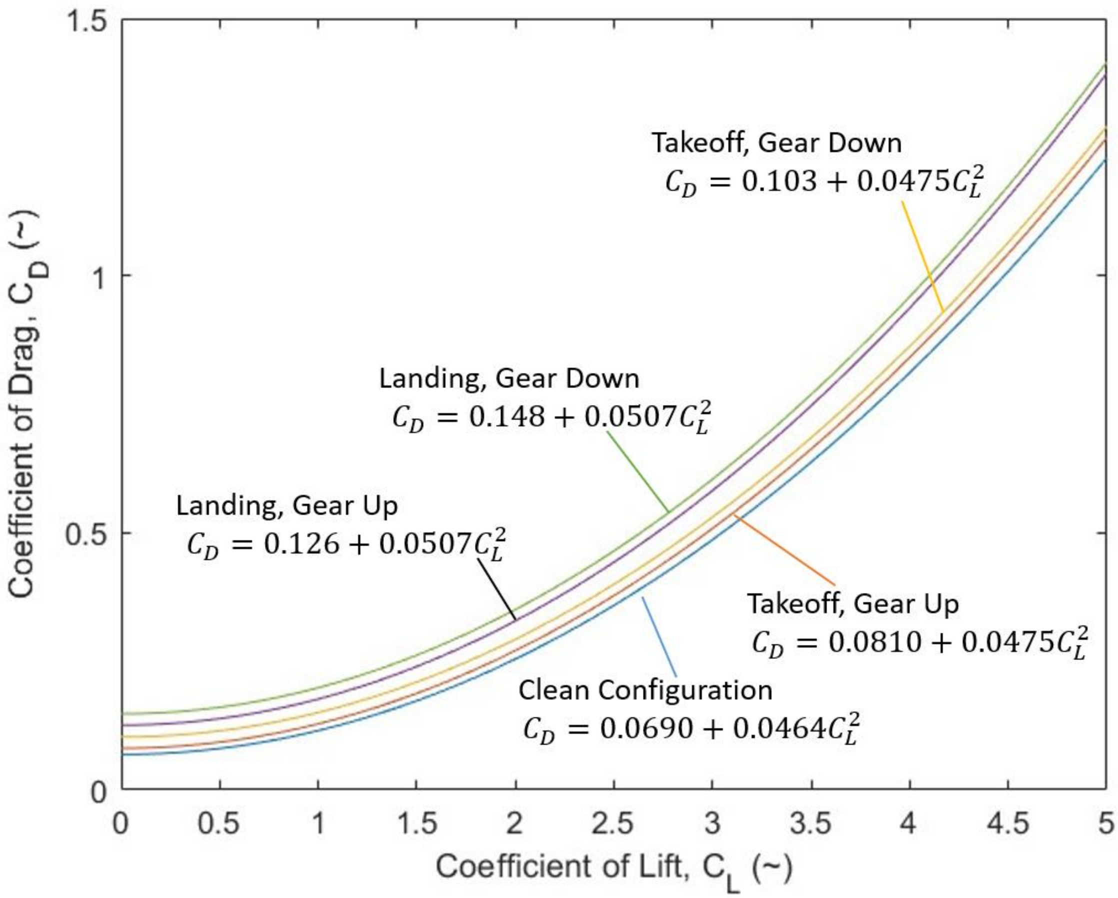

Figure 8.2: Wing Drag Polars

These drag polars were obtained by obtaining the total wetted area of all surfaces on the aircraft. These areas were obtained by visually finding the exposed area and using that to calculate the wetted area. Siemens NX was also used to verify these areas based on a three-dimensional model of the aircraft. The fuselage wetted area was found by utilizing a perimeter plot. This perimeter plot can be seen in Figure 8.3 below.

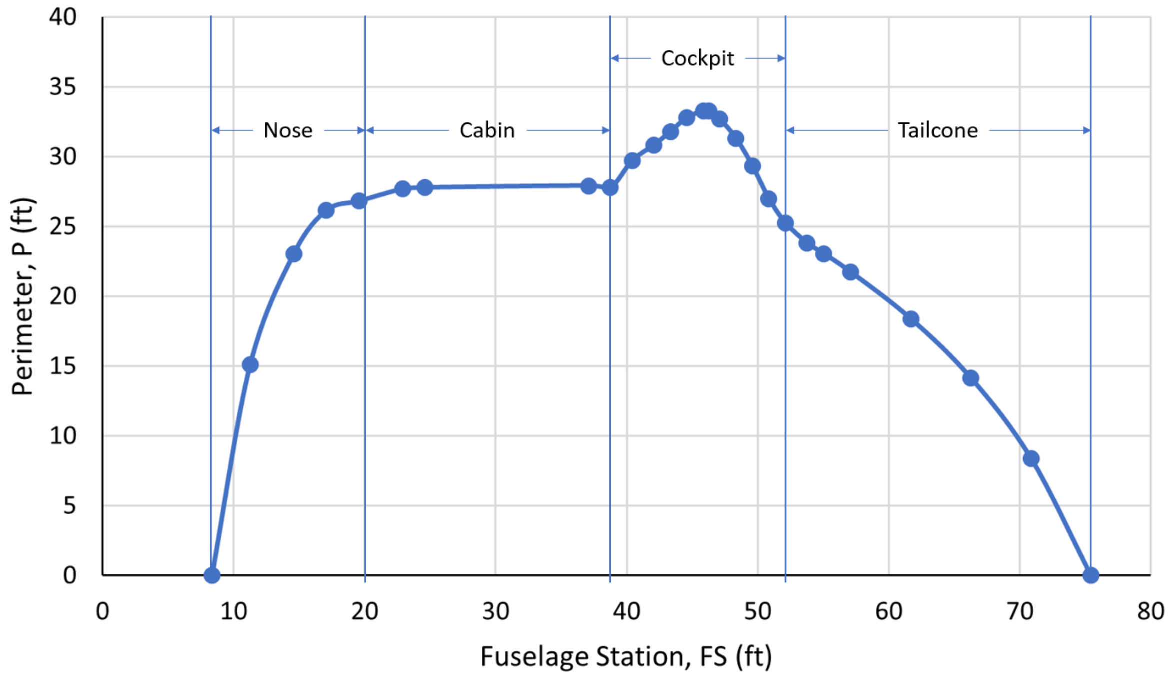

Figure 8.3: Fuselage Perimeter Plot

The area under this curve is the wetted area of the fuselage. The resulting drag polars are the updated, more accurate drag polars. Drag polars had been previously calculated based on Class I design before being updated. The various characteristics resulting from the original and updated drag polars can be seen in Table 8.1.

Table 8.1: Drag Characteristics

Characteristic	Old	New
C_{D_0}	0.0398	0.0356
C_f	0.007	0.007
Aspect Ratio	4.83	8.37
$\frac{L}{D}\Big\|_{max}$	8.84	12.3

The updated $\frac{L}{D}\Big|_{max}$ value does not account for the additional drag resulting from the boat hull of the fuselage. To accommodate that, the skin friction coefficient is raised from 0.007 to 0.013. This leads to an updated C_{D_0} value of 0.069 and ultimately results in an updated $\frac{L}{D}\Big|_{max}$ value of 8.84. This increase in the skin friction coefficient also accounts for the dirty conditions that the Frog Hopper will be subject to.

9 Advanced Technologies and Design Concepts

This section discusses the advanced technologies in this aircraft. For this aircraft, the major advanced technology is the detachable wings that allow this aircraft to be interoperable as a WIG. The free flight aircraft configuration will be known as the Frog Hopper-100FF and the WIG configuration is the Frog Hopper-100W.

9.1 Heilmeier's Catechism for Advanced Technology for Detachable Wings

Table 9.1.1: Heilmeier's Catechism for Advanced Technology

What is it called?	Detachable Wings
What are we trying to do?	Allow the aircraft to be interoperable as an amphibious aircraft and a WIG.
How does this currently get done?	• Smaller wing tip extensions to increase aircraft lift and reduce water landing loads • Folding wings to fit into gates
What limits present approaches?	The major limitation of current approaches is that the necessary connection structure for detachable wings can cause a significant increase in empty weight.
What is new about our approach?	The weight limitation can be mitigated by using composites as a major structure in the aircraft. This will cause a decrease in empty weight that will help offset the impact of the connection point.
Why, at this time, can our approach succeed?	There has been major growth in the use of composites in load-bearing structures in aircraft. Additionally, there is higher demand for travel now than ever before. This increased demand for shorter routes will result in lower life-cycle costs for this aircraft.

Table 9.1.2: Heilmeier's Catechism for Advanced Technology Cont.

What difference does our approach offer?	The major difference of this approach is that the detachable wings will essentially make the aircraft into a different vehicle. By switching the wings, the vehicle switches from a WIG to an amphibious aircraft, adding significant versatility to the vehicle.
What are the "mid-term" and "final exams?"	Mid-Term: Structural testing on both wings to ensure the connection joint can handle potential loads that may be faced. Final Exam: Flight test vehicle as a WIG and an amphibious aircraft. Test necessary time to switch wings.
How much will our approach cost?	The initial cost of this approach will be higher than making a more traditional amphibious aircraft out of composite material. The increased variety of routes that are able to be offered due to the versatility of the vehicle will result in a decrease in life cycle and acquisition costs, leading this to ultimately lower cost over time.

10 V-n Diagram

A V-n diagram is made to examine the loads on the aircraft at different velocities and different gust conditions. The V-n diagram (which combines gust lines with the maneuver diagram) can be seen below along with the relevant velocities.

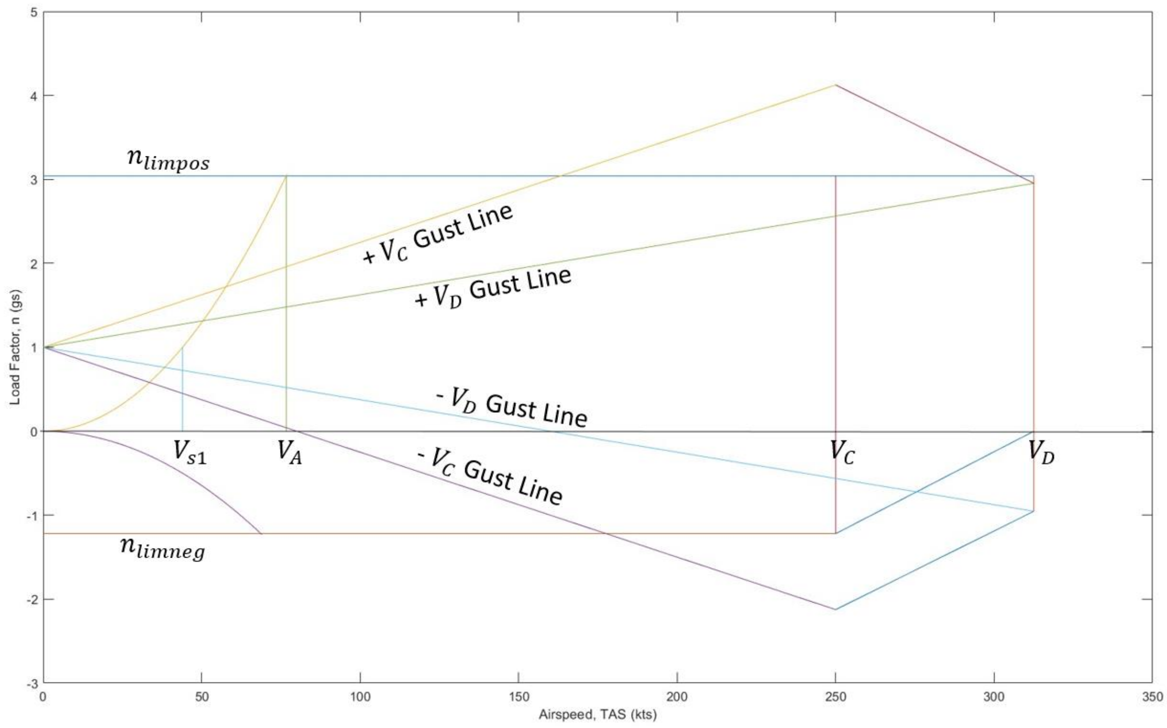

Figure 10.1: V-n Maneuver Chart

Table 10.1: V-n Maneuver Chart Relevant Velocities

Airspeed	Value (kts)
V_{s1}	44.0
V_A	76.7
V_C	250
V_D	312.5

11 Class I Cockpit and Fuselage Sizing

The cockpit of the Frog Hopper is suited for one pilot as specified in the RFP. In order to allow for a wide range in the size of the pilot, the cockpit is sized for both a 95th percentile man and a 20th percentile woman. The cockpit layout with both of these pilots can be seen in Figure 11.1 and Figure 11.2 below.

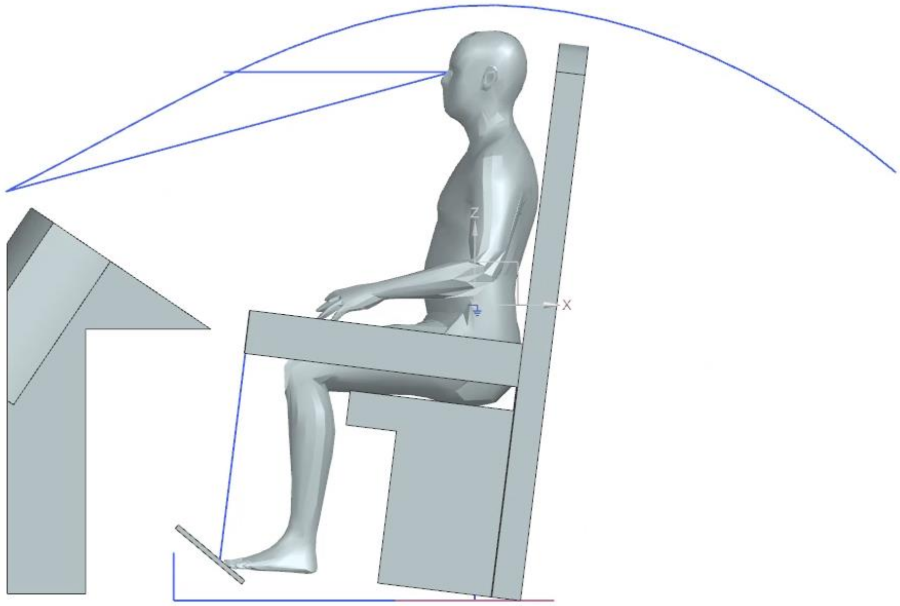

Figure 11.1: Cockpit Sideview (95th Percentile Male)

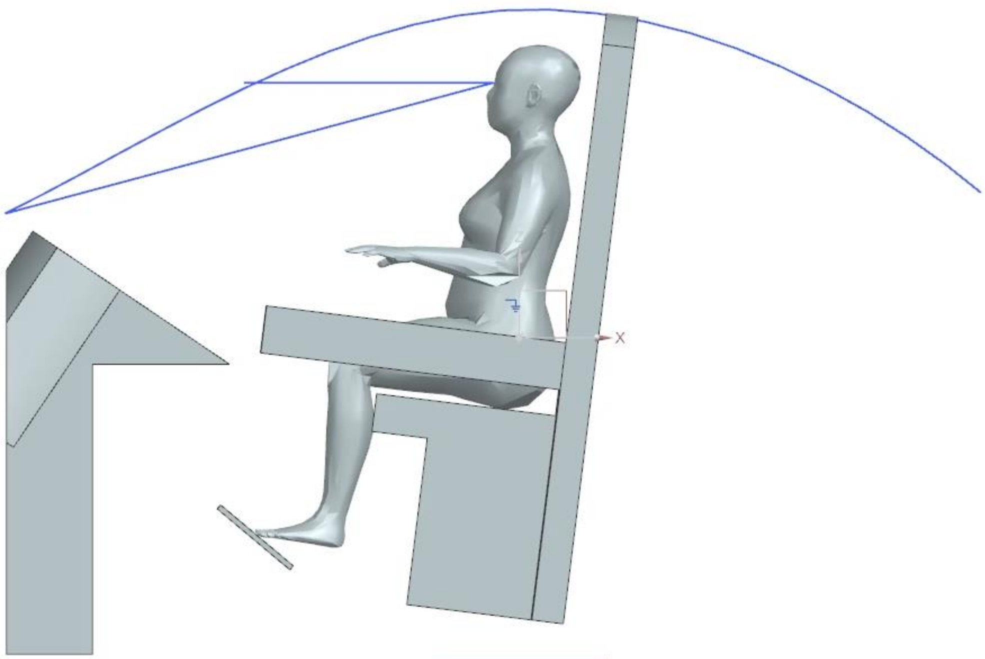

Figure 11.2: Cockpit Sideview (20th Percentile Female)

Stick controls are used in each armrest of the pilot’s seat for this aircraft. The seat and pedals are adjustable so that a 5’2” woman would be able to fly as well as a 6’3” tall man. The pilots’ eyes are collocated so that every pilot has the same view out of the cockpit. The cockpit sits in a pod above the fuselage to allow for increased vision laterally. Due to the WIG configuration, this increased range of visibility is extremely important. While in WIG flight or taking off in the free flight configuration, the pilot will be able to examine any hazards approaching the flight path that would not be seen otherwise and adjust accordingly. The extended cabin does not allow for the 15° of visibility that is required. Due to this, synthetic vision will be used in the cockpit. With an entry into service date of 2031, it is extremely feasible that synthetic vision is a relatively inexpensive addition to the cockpit. This addition is worth it for the added range of visibility. The cabin is arranged in ten rows of bench seating, with each row seating two people. The last row only has one seat, with the empty space next to it available for wheelchairs to lock into place. This allows for an increase in the comfort level of any passengers that use a wheelchair by not requiring a transfer into the airplane seat. 30” of pitch was used between seats to allow room for growth of humans as time goes on. A sideview of the general layout of the cabin and cockpit can be seen in Figure 11.3 below.

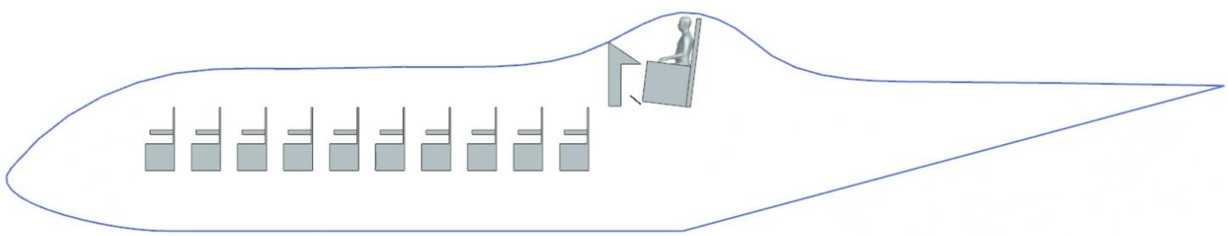

Figure 11.3: Fuselage Sideview

Once the layout inside the fuselage was determined, a skin could be wrapped around the outside. This results in a fuselage with a fineness ratio of 7.57.

The fuselage profile can be seen in Figure 11.4 below.

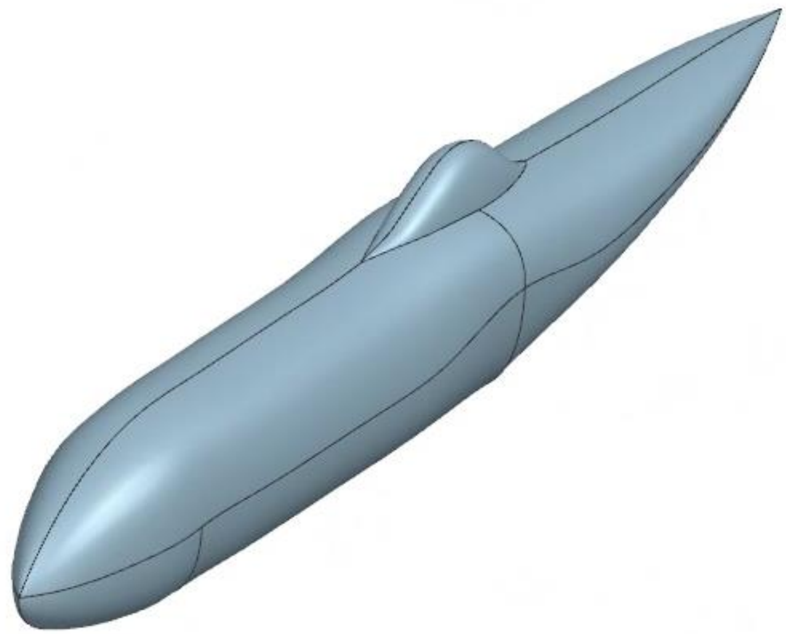

Figure 11.4: Fuselage Profile

12 Class I Engine Installation

A PT6A-68B engine was chosen for the turboprop engines on the Frog Hopper. The main advantage of the PT6A line of engines is that they have significant foreign object damage (FOD) resistance. The Frog Hopper will be taking off from water, dirt, grass, and gravel surfaces in addition to more traditional runways. This fact in addition to the location of the engines being close to the ground suggests that there is likely to be FOD affecting the engines. This leads to a FOD resistant engine being extremely important. Characteristics of the PT6A-68B engine can be seen in Table 12.1 below.

Figure 12.1: PT6A-68B Engine Characteristics

Characteristic	Value
Power	1,600 hp
Specific Fuel Consumption	$0.54 \frac{lb}{hp*hr}$
Diameter	19 in
Length	72.2 in
Weight	575 lb

The power for this engine means that having two of these engines on the Frog Hopper will meet the power requirement. The engines are ducted for both the aerodynamic benefit and the additional passenger safety. With the engines being located at a lower waterline, ducting the engine helps mitigate the risk of people impacting the engine and propeller at any point. The duct is extremely short at 7.36 inches. Chevrons are then added to the duct to mitigate any noise from the engine. This will improve the experience for both the passengers flying as well as the people that the Frog Hopper is flown over. Due to the amphibious nature of the aircraft and the potential for WIG operation, there is a significant risk of bird strike to the engines. To help mitigate this, a cage is placed around the front of the engine inlets. This results in protection from birds flying into the engine without greatly affecting the inlet flow. Basic models of the engine both unducted and ducted can be seen in Figure 12.1 and Figure 12.2 below.

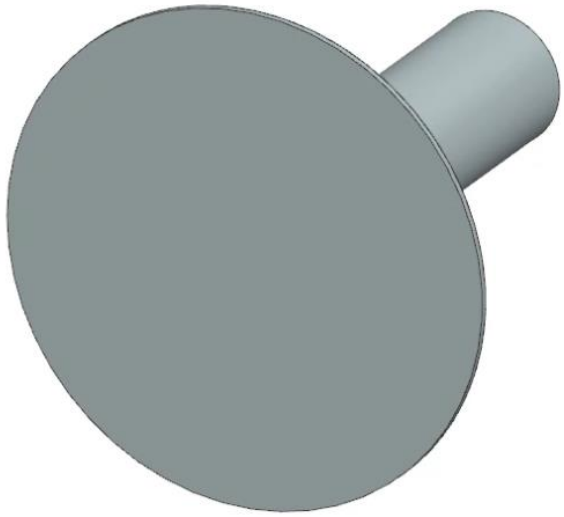

Figure 12.1: Engine Unducted

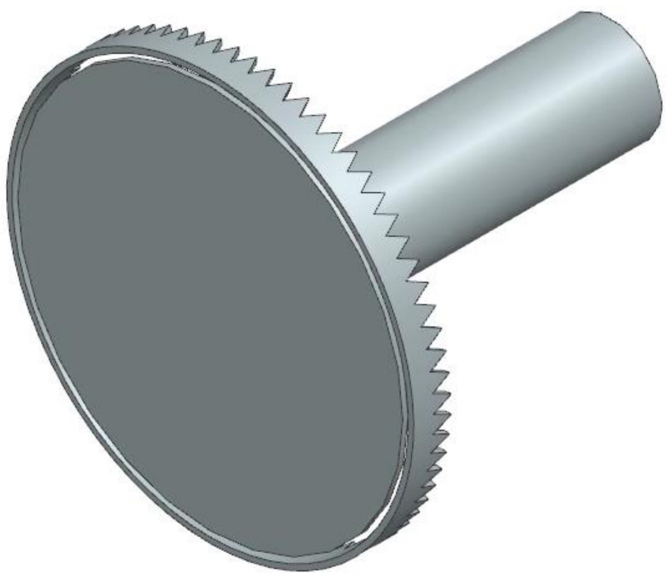

Figure 12.2: Engine with Duct

13 Class I Wing Layout Design

Wing layout design has to be undergone for both the WIG wing and the free flight wing. The free flight wing configuration took inspiration from the Boeing 314-A and existing WIGs such as the RBF X-113 or the design in Reference 25. This resulted in a wing with both a distinct inboard and outboard section. The De Havilland Canada DHC-6 Twin Otter was also considered and used as the driving factor behind the span of the wing. The Twin Otter is a similar size to the Frog Hopper, so having a similar span is reasonable. The WIG wing on the other hand is largely based on WIGs designed by Alexander Lippisch as well as the BATWinG design in Reference 25. The tips of the WIG wing have an anhedral characteristic, which is necessary to help trap air underneath the wings in WIG flight. The specific characteristics of both wings can be found later on in the list of salient characteristics in Chapter 19. The designed WIG wing and free flight wing can be seen in Figure 13.1 and Figure 13.2 below.

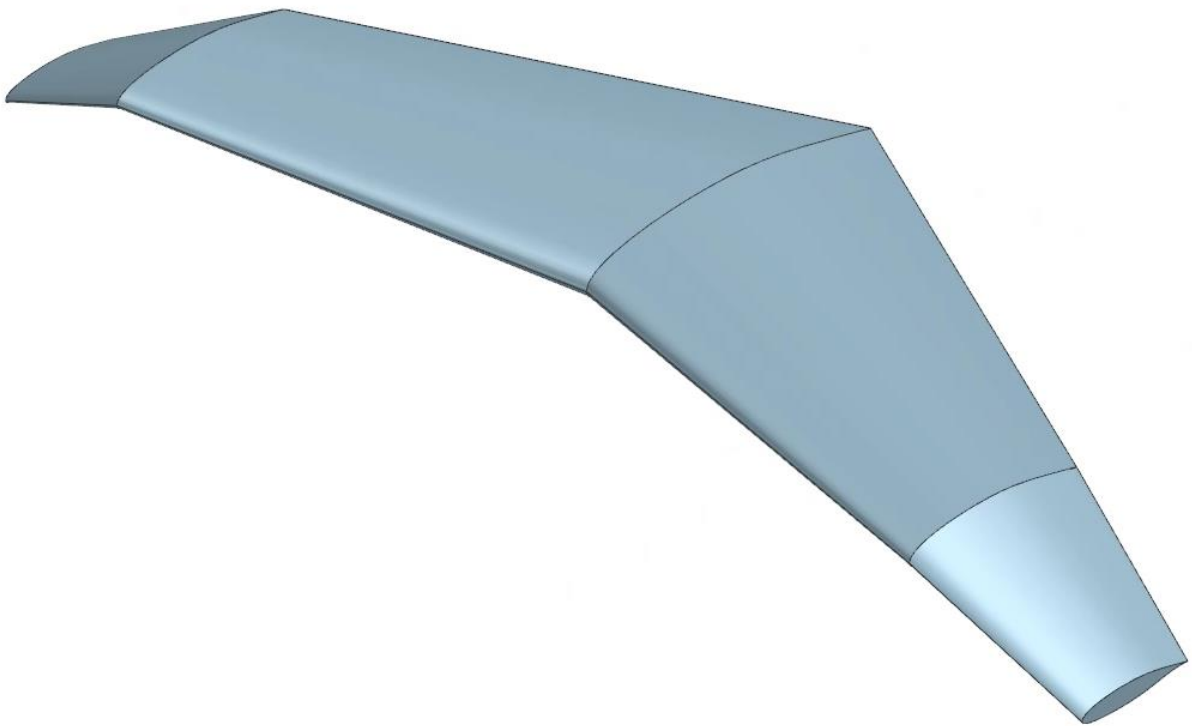

Figure 13.1: WIG Wing Model

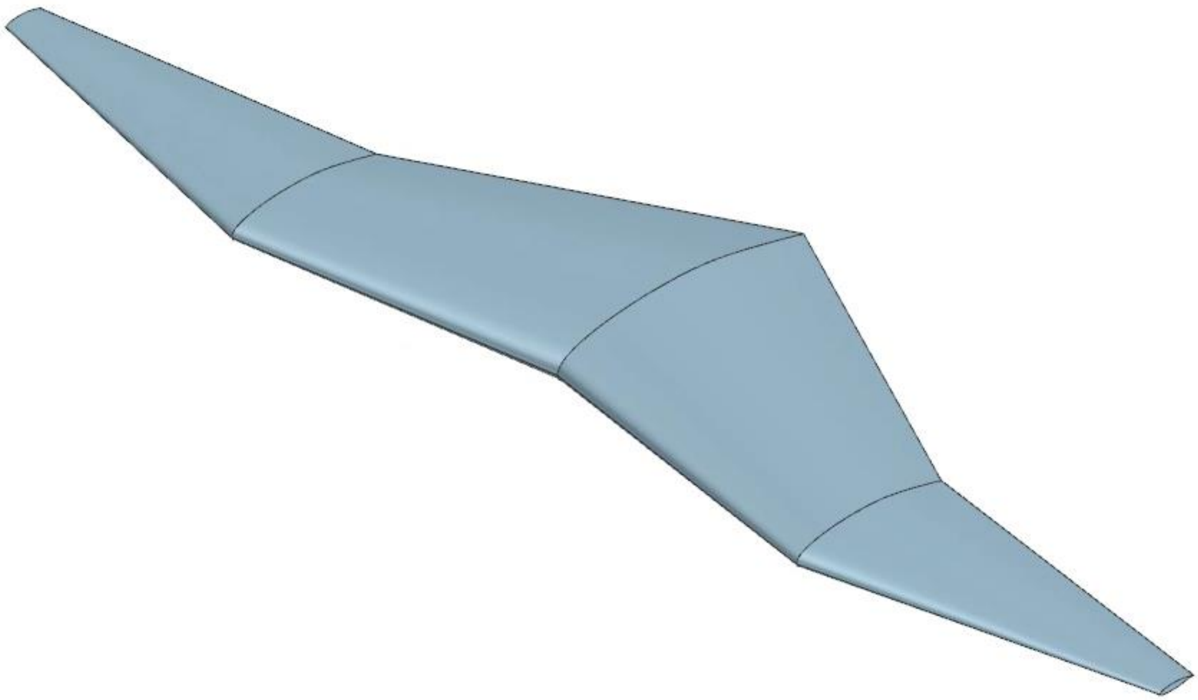

Figure 6.2: Free Flight Wing Model

14 Class I Flight Control Device Sizing

The flight control devices on the aircraft had to be sized. This was done by considering the necessary coefficient of lift on the wing, elevator, and vertical tail in takeoff, cruise, and landing. The flight control devices on the Frog Hopper are inboard and outboard flaperons, an elevator, and a rudder. This allows for roll, pitch, and yaw control for the aircraft. The calculated sizes of these devices are listed later in the list of salient characteristics for the aircraft in Chapter 19.

15 Class I Empennage Sizing

The Frog Hopper has its empennage in a T-tail configuration. This configuration was chosen for several reasons. One reason this configuration was chosen is that due to this aircraft being amphibious, a T-tail keeps the horizontal tail out of the water. This will increase the horizontal tail's effectiveness and reduce fatigue on the component. Additionally, the vertical tail has to be kept out of the wake of the engines to maintain its effectiveness. With a dual engine design, this leads to a T-tail being a very strong configuration. The empennage components were sized from tail volume coefficients. The tail volume coefficients were based on historical data from the Canadair CL-215. The specific characteristics of the empennage can be seen later in the list of salient characteristics in Chapter 19. The horizontal and vertical tail can be seen in Figure 15.1 and Figure 15.2 below.

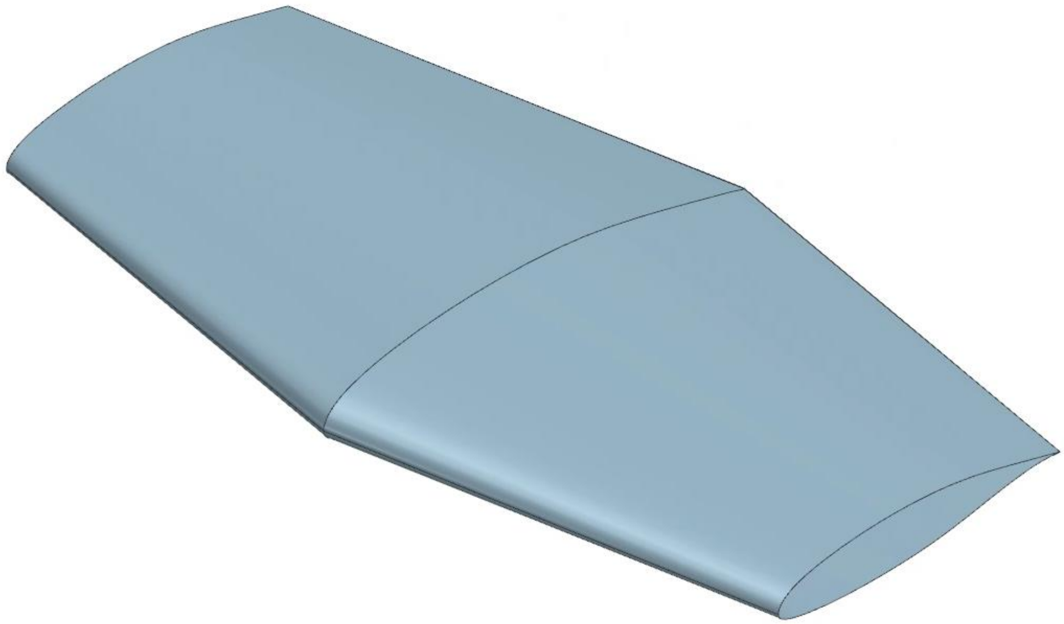

Figure 15.1: Horizontal Tail Model

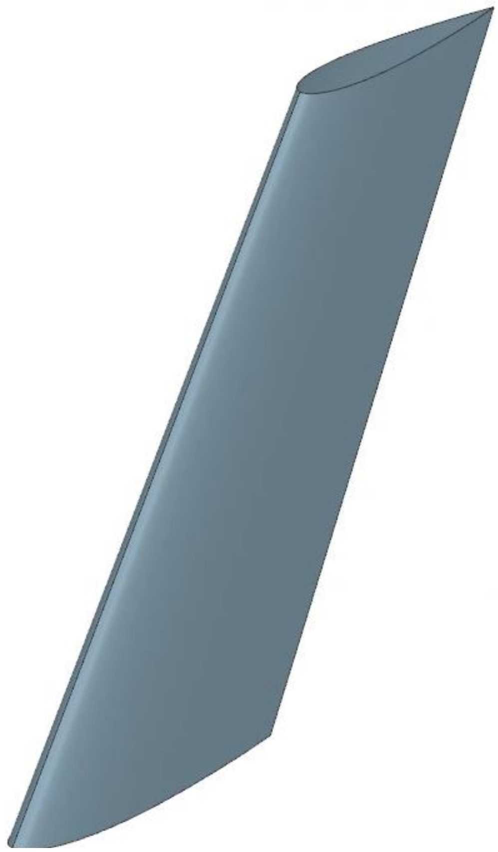

Figure 15.2: Vertical Tail Model

16 Class I Landing Gear Sizing

The initial sizing of the landing gear allows for the landing gear placement to be determined. The landing gear are in the conventional configuration with a nose gear and two main gear. The landing gear is retractable to avoid additional drag penalties in cruise flight. The landing gear is located such that the main gear takes 90% of the load and the nose gear takes 10% of the load. This results in the main gear being located at fuselage station (FS) 472 and the nose gear being located at FS 172. The landing gear location can be seen in Figure 16.1 below.

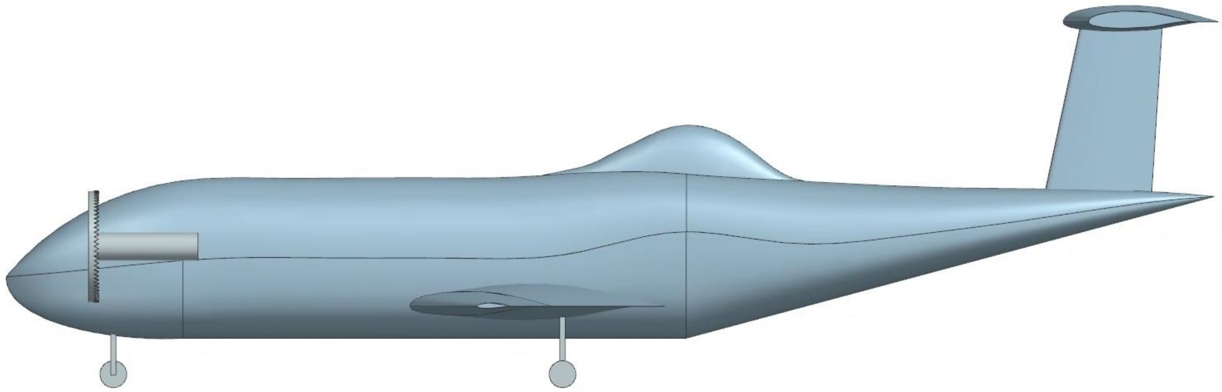

Figure 16.1: Aircraft Side View with Landing Gear

A lateral ground clearance of greater than 15° and a rotation of greater than 5° are necessary for the landing gear placement. Once these are satisfied, lateral tip over is verified by expanding a cone from the aircraft's center of gravity. This verification can be seen in Figure 16.2 below.

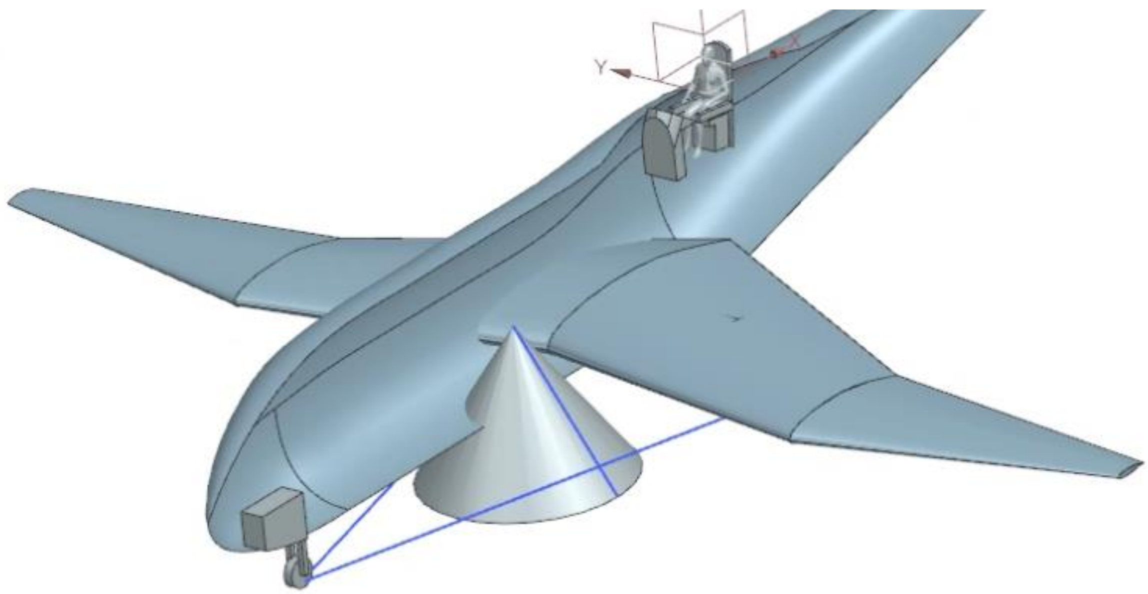

Figure 9.2: Lateral Tip-Over Verification

Since the cone is within the triangle created by the landing gear on the ground plane, it satisfies lateral tip over.

17 Class II Landing Gear Sizing

Class II sizing was undergone on the landing gear of the aircraft. The first thing done was calculating the vertical touchdown rate, w_t. This is done using the equation $w_t = 4.4 * \sqrt[4]{\frac{W}{S}\Big|_L}$. This resulted in a vertical touchdown rate of 10.4 ft/s. This is outside of the 7-10 ft/s range used for FAR 23, so a vertical touchdown rate of 10 ft/s is used. The dynamic load was then calculated for the tires of the main gear and the nose gear. This resulted in a dynamic load of 2,100 lb for the nose gear tires and 2825 lb for the main gear tires. Both the nose gear and main gear were assumed to be in a dual configuration initially.

Additionally, type III tires were chosen as a low-pressure tire is necessary for the surfaces that the aircraft will take off from. The static load on each tire was then found by dividing the dynamic load by 1.45. This resulted in a static load for the nose tires of 1448 lb and a static load for the main tires of 1948 lb. These static loads need to be compared to the original loads calculated for the tires, being 775 lb for the nose tires and 3488 lb for the main tires. The larger static loads are the ones that are considered. The maximum velocity of the tire is then calculated by calculating the landing velocity (91.2 ft/s) by 1.2. This results in a maximum landing velocity of 109 ft/s. The tires can't have a pressure greater than 35 psi due to the conditions that the aircraft may take off from. No tire was found that could satisfy all of these criteria, so the main landing gear configuration was changed to tandem twin. This results in four tires on each of the main struts, leading to a static load of 1744 lb on each of the main gear wheels. This resulted in downselecting to two tire options that both satisfied the criteria. The lighter and smaller tire is the one that was chosen. Once the tire was chosen, the allowable tire deflection can be calculated from the outside tire diameter and the loaded radius. The struts of the main gear and nose gear were then sized using the vertical touchdown rate, the landing weight of the aircraft, the allowable tire deflection, the load on the strut, the landing gear load factor, and the energy absorption efficiency. Oleo-pneumatic shock absorbers are used for the landing gear because of their energy absorption capabilities. Once the stroke and diameters were calculated for the landing gear struts, a brake system was specified. Carbon-carbon antilock brakes are chosen to be used in this landing gear system as they are very effective and will allow for short landing lengths. Tire and landing gear characteristics can be seen in Table 11.1 below.

Table 11.1: Landing Gear Characteristics

Characteristic	Value
Tire Type	Type III
Tire Size	8”-6”
Tire Maximum Load	2,050 lb
Tire Pressure	35 psi
Tire Weight	11 lb
Outside Tire Diameter	19.5”
Tire Loaded Radius	7.5”
Allowable Tire Deflection	2.25”
Energy Absorption	0.8
Landing Gear Load Factor	3.0
Main Gear Strut Stroke	6.95”
Nose Gear Strut Stroke	6.51”
Main Gear Strut Diameter	3”
Nose Gear Strut Diameter	2.11”

The resulting main gear and nose gear can be seen in Figure 11.1 and Figure 11.2 below.

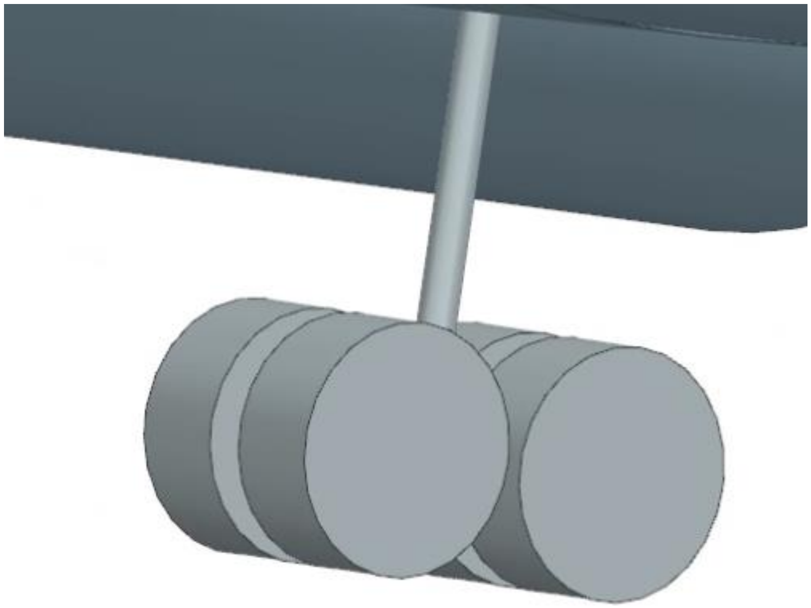

Figure 11.1: Main Gear Model

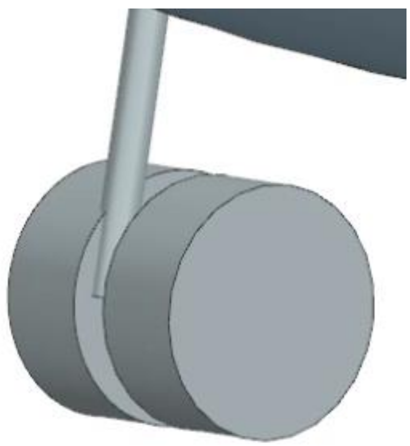

Figure 11.2: Nose Gear Model

It’s important to note that the struts for the landing gear are connected to the wheels in the forward portion of the landing gear such that the landing gear is dynamically stable. The necessary tire clearance for the landing gear bays were then calculated. This results in a clearance of 1.32” in the width direction and 2.9” in the radial direction. This results in the main gear bay and nose gear bay as can be seen below.

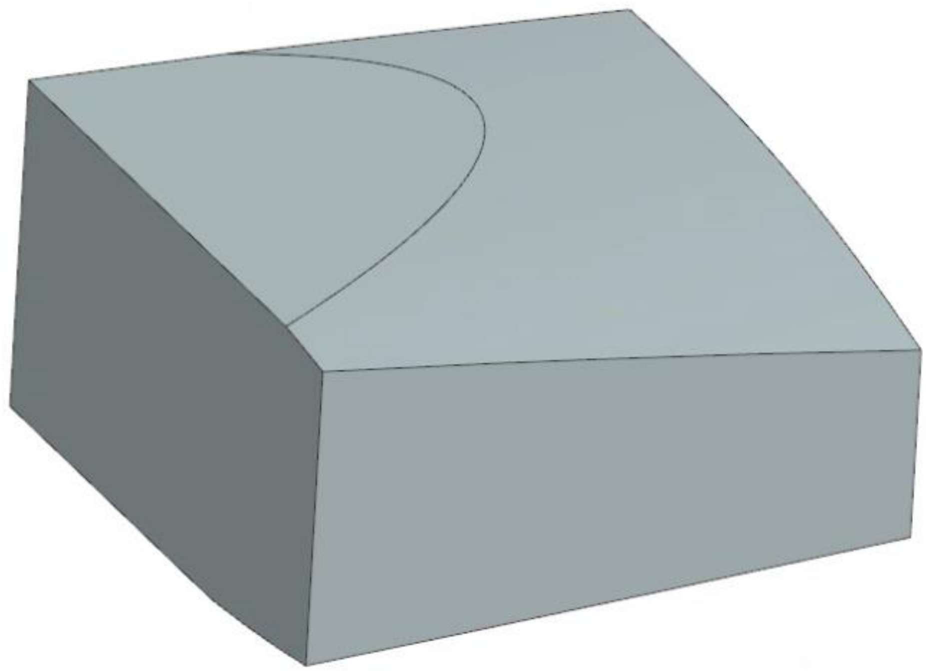

Figure 11.3: Main Gear Bay Model

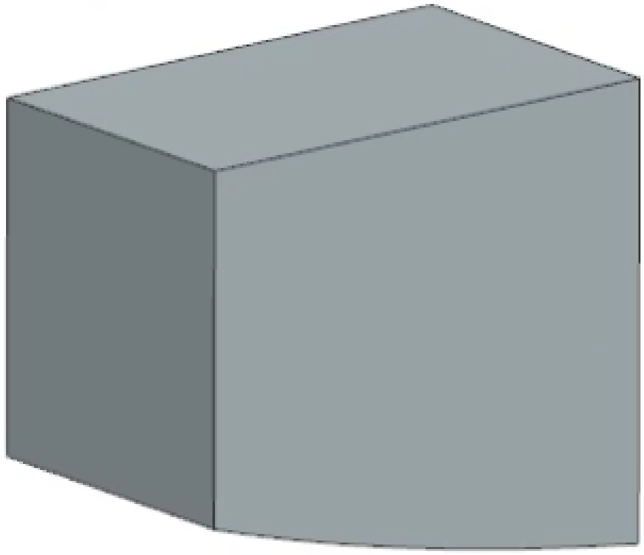

Figure 11.4: Nose Gear Bay Model

The main gear bays are located in the wings of the aircraft, while the nose gear bay is located in the nose of the fuselage. Both the free flight wings and WIG wings are similarly sized inboard, resulting in the same dimensioned main gear bay fitting in both. The nose gear deploys from the forward towards the aft of the aircraft. The main gear deployment is slightly more complicated. Due to the tandem twin configuration of the wheels being necessary, the radii of the wheels cannot fit parallel to the body z-axis in the wing. This results in the gear needing to rotate 90 degrees before being deployed or retracted, such that the sides of the wheels are parallel to the body x-y plane. This added rotation adds complexity to the landing gear but is necessary for the main gear to fit in the wing. Similarly to the nose gear, the main gear deploy from forward to aft. This direction of deployment is so that the gear is locked in the deployed position from the aircraft's momentum in the event of a hydraulic system failure. For the same reason, springs will be used to mechanically force the main gear to the correct orientation. Accounting for failure in the hydraulics for the landing gear will increase the safety of the system, as the hydraulic system lacks redundancies. The locations of the landing gear bays can be seen in Figure 11.5 below.

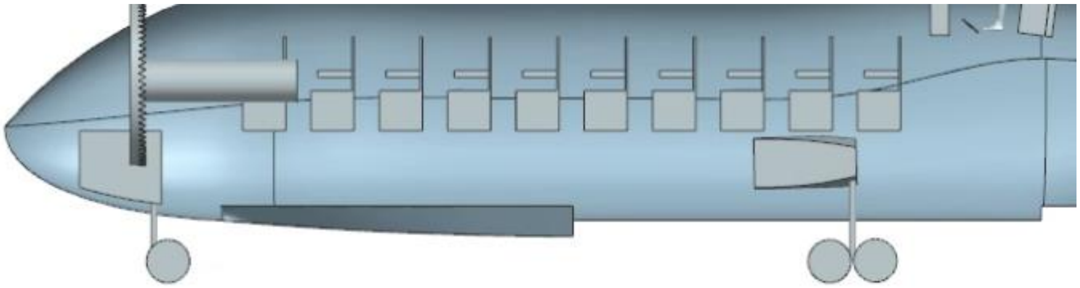

Figure 11.5: Landing Gear Bay Locations

18 Amphibious Characteristics

Several adjustments had to be made due to the aircraft being amphibious. Firstly, a buoyancy check needed to be done to ensure that there was enough air below the waterline to allow the aircraft to float. The necessary volume of air was calculated using the equation $V_{air} = \frac{W_{to}}{\rho_{H2O}} = \frac{15{,}500\ lb}{62.4\frac{lb}{ft^3}} = 248\ ft^3$. With the original placement of the wings, there was a calculated volume of air of 235 ft^3. Since only 15 ft^3 more of volume was necessary, the wings were moved up 1”. This small change resulted in a volume of air of 265 ft^3, which satisfies the buoyancy requirement. This section of the fuselage can be seen below in Figure 18.1.

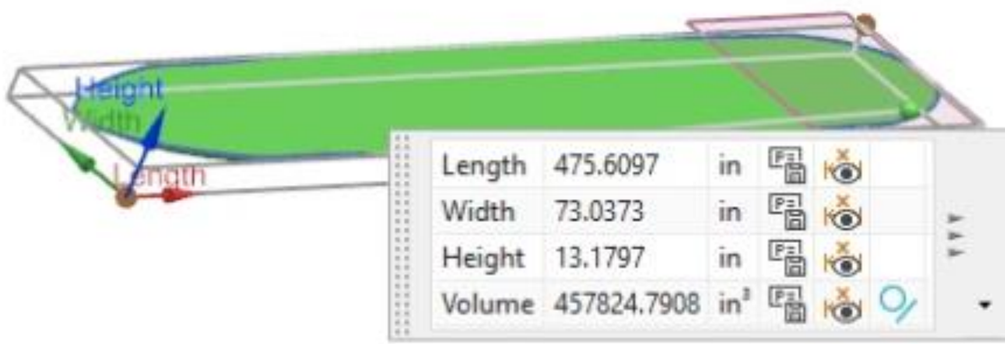

Figure 14.1: Buoyancy Air Volume

Additionally, two steps need to be added in the bottom of the fuselage to allow for separation from the water during takeoff. The forward step was created by adding material to the fuselage, while the aft step was created by taking a cut out at the start of the tail cone. These steps in the fuselage are necessary as they provide a means of interrupting the adhesive properties of the water. This results in the water flowing freely behind the steps and minimum skin friction so the aircraft can lift out of the water. The two steps are located forward and aft of the Frog Hopper’s center of gravity, allowing the aircraft to rotate into a pitch-up attitude quickly. These steps can be seen in Figure 18.2 below.

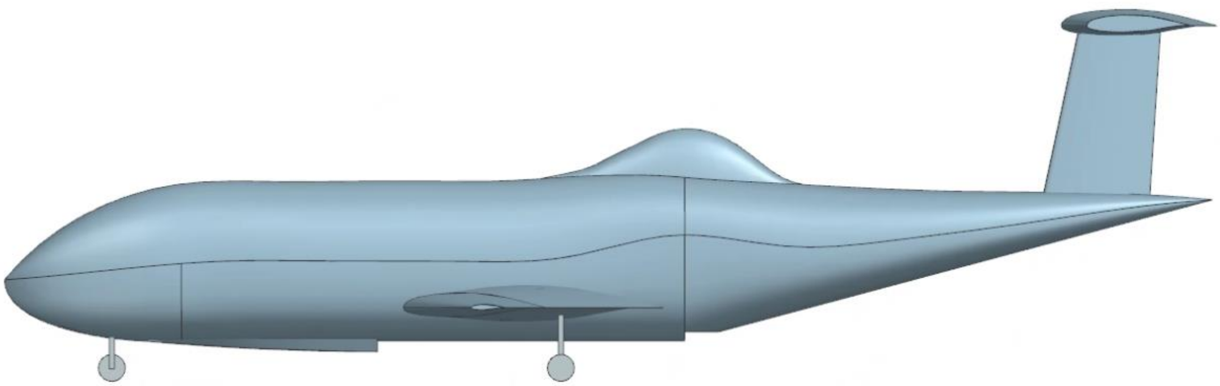

Figure 18.2: Fuselage Steps

Lastly, floats had to be added to the wings to allow for roll stability on the water. This is done to help achieve being able to take off and land from sea state 3. An image of the float, as well as the float's location can be seen in Figure 18.3 and Figure 18.4 below.

Figure 18.3: Frog Hopper Float

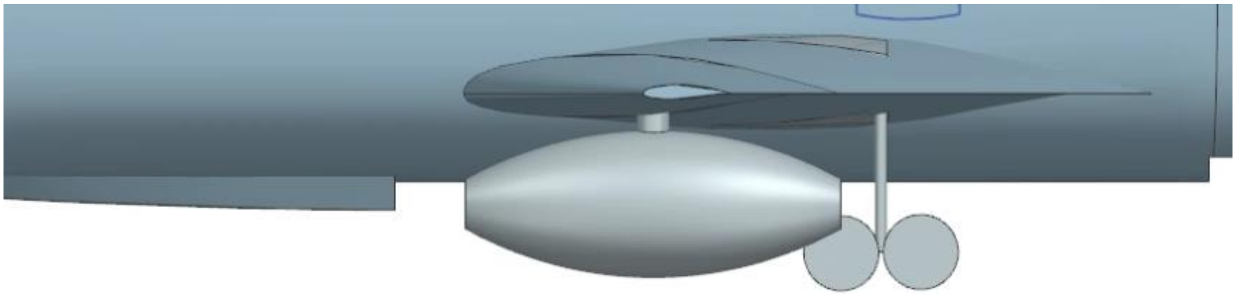

Figure 18.4: Frog Hopper Float Location

19 Aircraft Three-View and List of Salient Characteristics

The three views of both the Frog Hopper-100FF configuration and the Frog Hopper-100W configuration can be seen in Figure 19.1 and Figure 19.2 below.

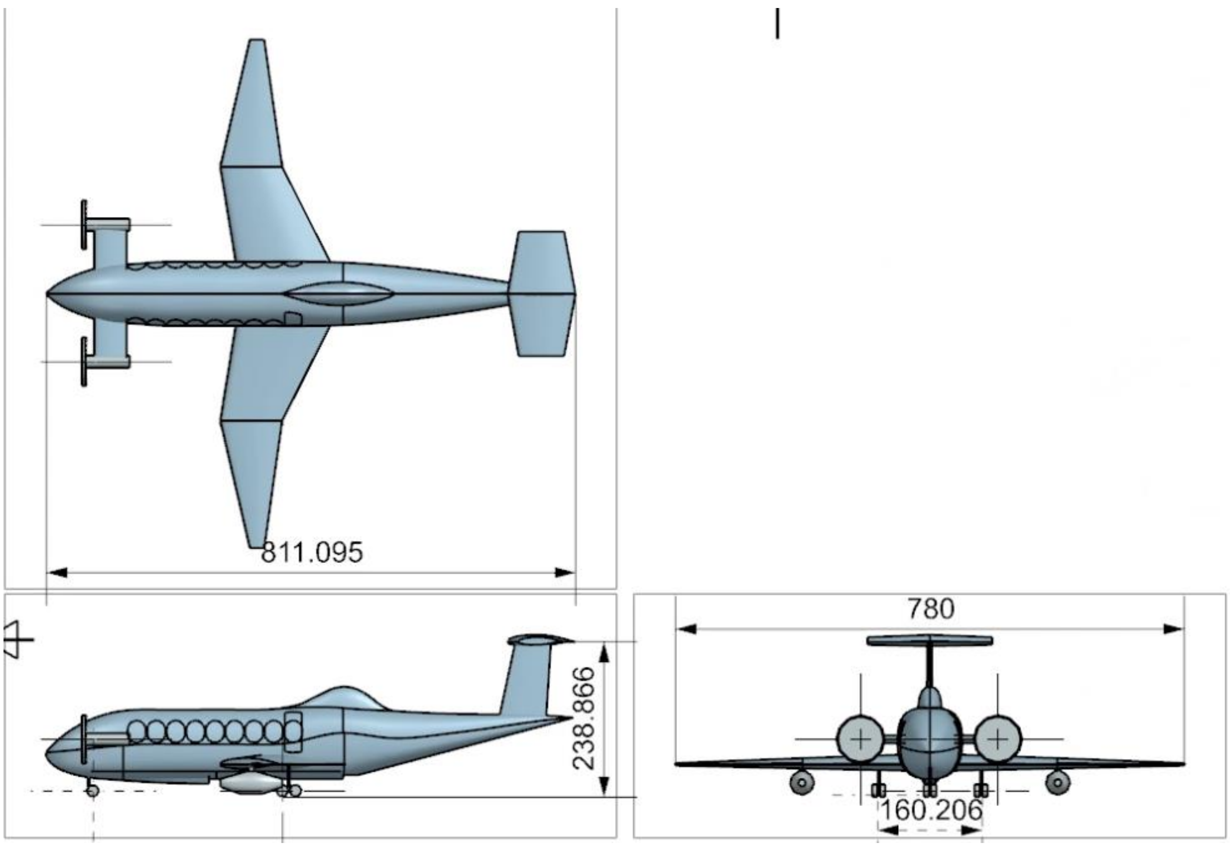

Figure 19.1: Frog Hopper-100FF 3-View

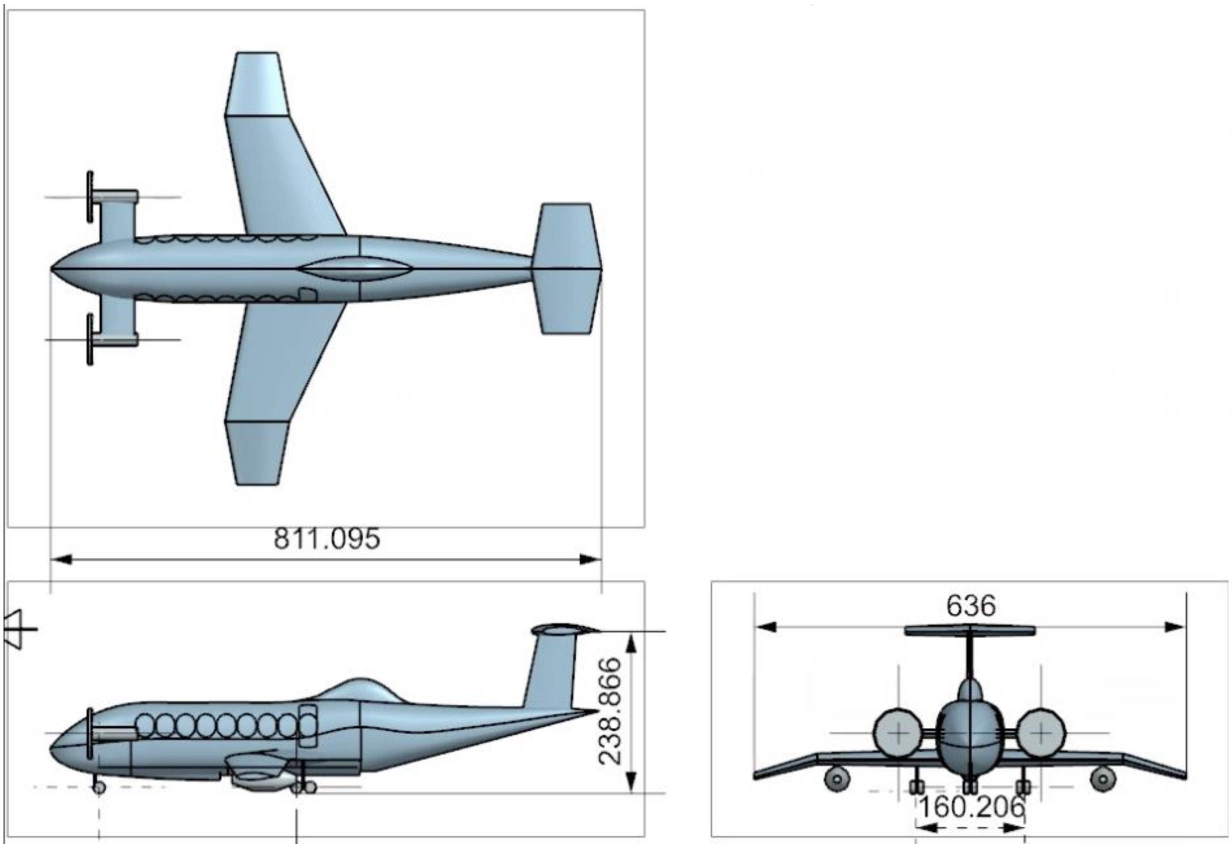

Figure 19.2: Frog Hopper-100W 3-View

The list of salient characteristics is an important entity for an aircraft. It collects much of the important information about the various components of the aircraft in one place. The list of salient characteristics for the Frog Hopper can be seen in Table 19.1 below.

Table 19.1: List of Salient Characteristics

	Free Flight Wing	WIG Wing	Horizontal Tail	Vertical Tail
Area	505 ft^2	499 ft^2	115 ft^2	52.7 ft^2
Span	65 ft	53 ft	15.9 ft	10.0 ft
MGC	8.89 ft	9.26 ft	7.22 ft	5.29 ft
MGC LE FS	372.6 in	375 in	820 in	810 in
AR	8.37	5.63	2.2	1.9
First Segment Sweep Angle	-18.4° (c/2)	-18.4° (c/2)	5° (c/4)	10° (c/4)
Second Segment Sweep Angle	7.9° (c/4)	0° (c/2)	5° (c/4)	10° (c/4)
Taper Ratio	0.138	0.373	0.67	0.75
Thickness Ratio	0.17	0.17	0.17	0.12
Airfoil	LS-0417	LS-0417	LS-0417	NACA 0012
Dihedral	0°	0°/30°	0°	90°
Incidence Angle	0°	0°	0°	0°
Flaperon Chord Ratio	0.3	0.3		
Flaperon Span Ratio	0.124 to 0.897	0.124 to 0.897		
Elevator Chord Ratio			0.3	
Rudder Chord Ratio				0.3
	Fuselage	Cabin Interior	Full Aircraft	
Length	67.3 ft	26.7 ft	67.6 ft	
Max Height	11.8 ft	9.69 ft	12.9 ft	
Max Width	8.17 ft	8.17 ft	65 ft	

Isometric views of both the Frog Hopper-100FF and the Frog Hopper-100W are also taken. These show how many of the previously mentioned components are assembled in the aircraft. These isometric views can be seen in Figure 19.3 and Figure 19.4 below.

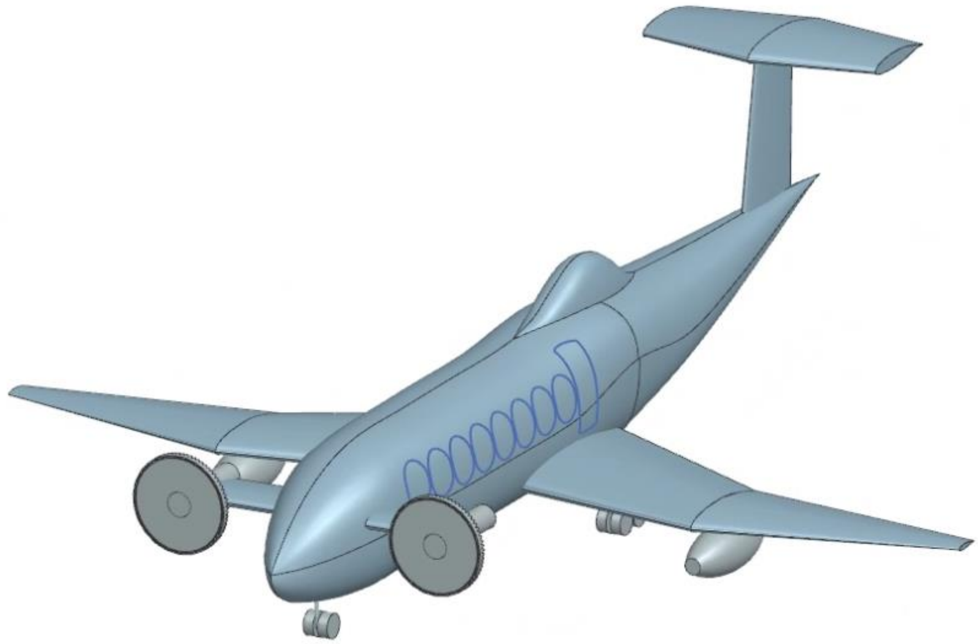

Figure 19.3: Frog Hopper-100FF Isometric View

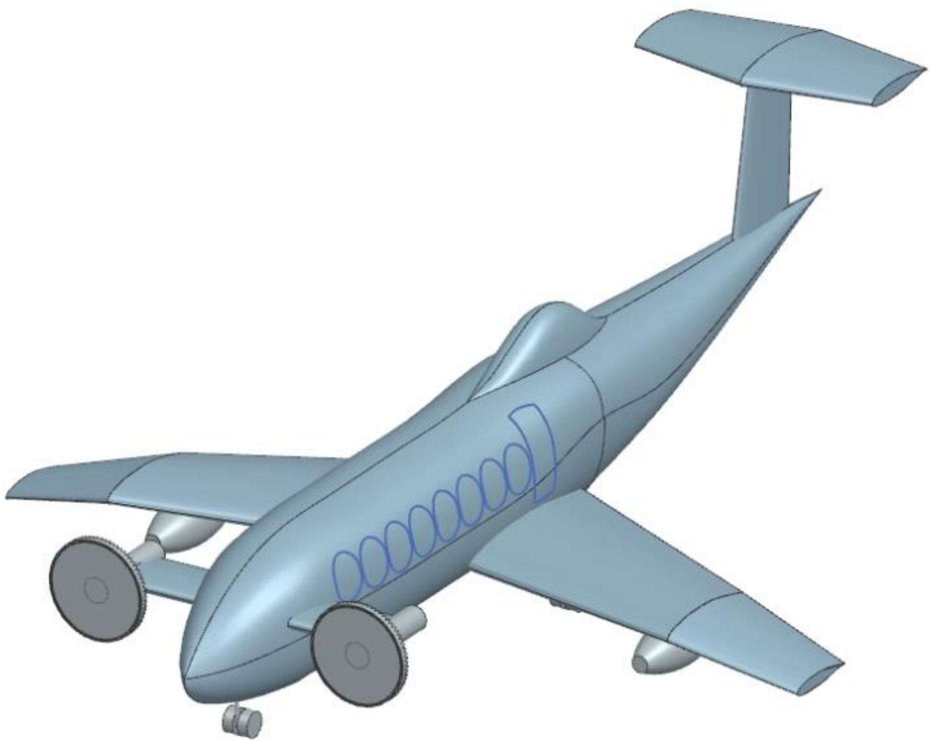

Figure 19.4: Frog Hopper-100W Isometric View

20 Class II Weight and Balance

Several weights on the aircraft are known from the request for proposal and existing documentation. These known weights can be found in Table 20.1 below.

Table 20.1: Aircraft Known Weights [1], [23]

Weight	Value (lb)
Payload (Passenger Mission)	4,389
Payload (Cargo Mission)	5,000
Crew	193.6
Engine	1,150
Fuel	1,566
Trapped Fuel and Oil	16

The remaining component weights of the aircraft were calculated using methods found in Reference 27. These weights can be seen in Table 20.2 and Table 20.3 below.

Table 20.2: Class II Calculated Weights [27]

Weight	Value (lb)
Wing	922
Horizontal Tail	123
Vertical Tail	56.6
Aerodynamic Engine Pylons	34.1
Fuselage	3,248
Duct	317
Landing Gear	622
Flight Control System	479
Hydraulic System	155
Electrical System	161
Instrumentation, Avionics, and Electronics	253

Table 20.3: Class II Calculated Weights Cont. [27]

Auxiliary Power Unit	132
Furnishings	823
Baggage and Cargo Handling Equipment	23
Auxiliary	87.3
Paint	70

These weights result in a fixed equipment weight of 2,183 lb and a takeoff weight of 15,430 lb for the cargo mission. The takeoff weight for the passenger mission is 14,819 lb due to the decrease in payload weight. These takeoff weights are within 0.5% of the Class I estimations that were made. The flight control system, hydraulic system, electrical system, instrumentation, avionics, electronics, auxiliary power unit, furnishings, baggage and cargo handling equipment, auxiliary, and paint weights make up the fixed equipment weight of the Frog Hopper. The resulting fixed equipment weight is 2,183 lb. Reference 27 was also used to determine center of gravity locations of various components. The center of gravity locations can be seen in Table 20.4 and Table 20.5 below.

Table 20.4: Component CG Locations

Component	Fuselage Station (in)
Crew	560
Passengers	348
Cargo (Passenger Mission)	390
Cargo (Cargo Mission)	432
Fixed Equipment	432
Engine	192
Fuel	368
Trapped Fuel and Oil	299
Wing	444
Horizontal Tail	861
Vertical Tail	851

Table 20.5: Component CG Locations Cont.

Aerodynamic Engine Pylons	192
Fuselage	314
Duct	159
Landing Gear	352

A CG excursion chart was then developed to examine where the center of gravity migrates depending on the non-permanent loads on the aircraft. This CG excursion chart can be seen in Figure 20.1 below.

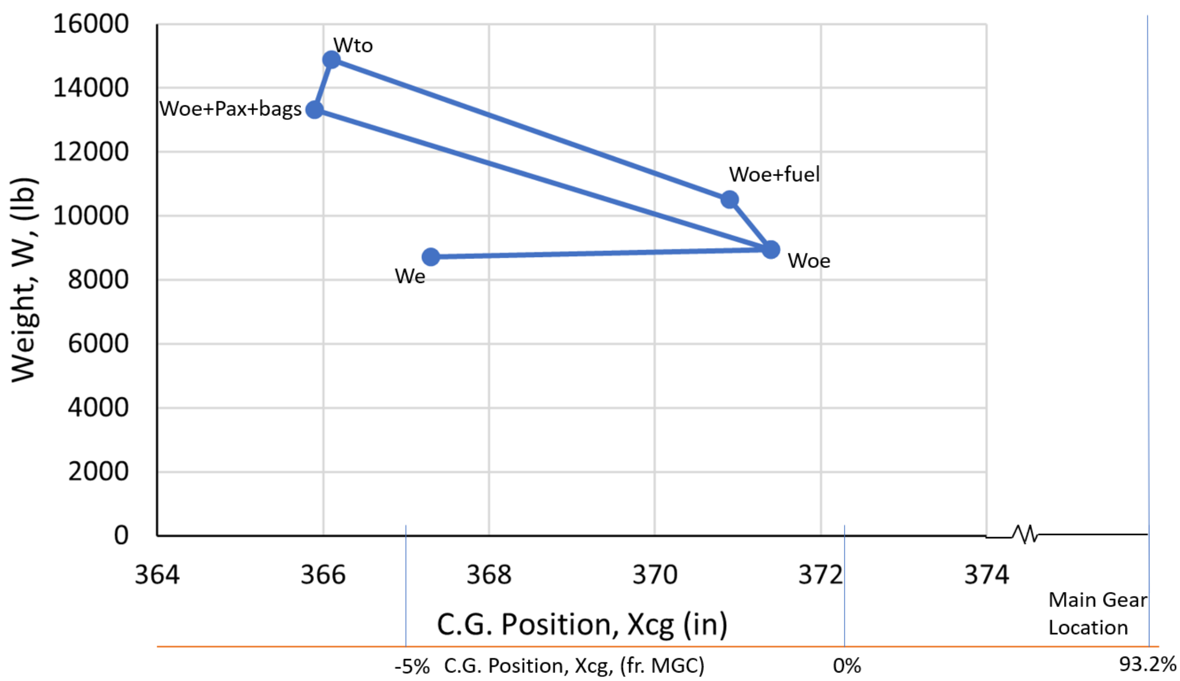

Figure 20.1: Frog Hopper CG Excursion Chart

21 Class I Stability and Control

Longitudinal stability and control analysis was performed. The ducts on the turboprop act as canards is the longitudinal stability of the system. After performing analysis with the ducts at their initial size, the aerodynamic center was in front of both the forward and aft CG of the system. To adjust this, the chord of the ducts are decreased to 10% of their initial size. This results in a static margin range of 5.5% to 19.1%. In addition to the ducts, the pylons that attach the engine to the fuselage are given an aerodynamic shape. The pylon has a NACA 0024 airfoil that can hold ballast tanks and provide aerodynamic support. Additionally, considering these tanks leads to a static margin range of 10.5% to 15.7%. The longitudinal x-plot can be seen in Figure 21.1 below.

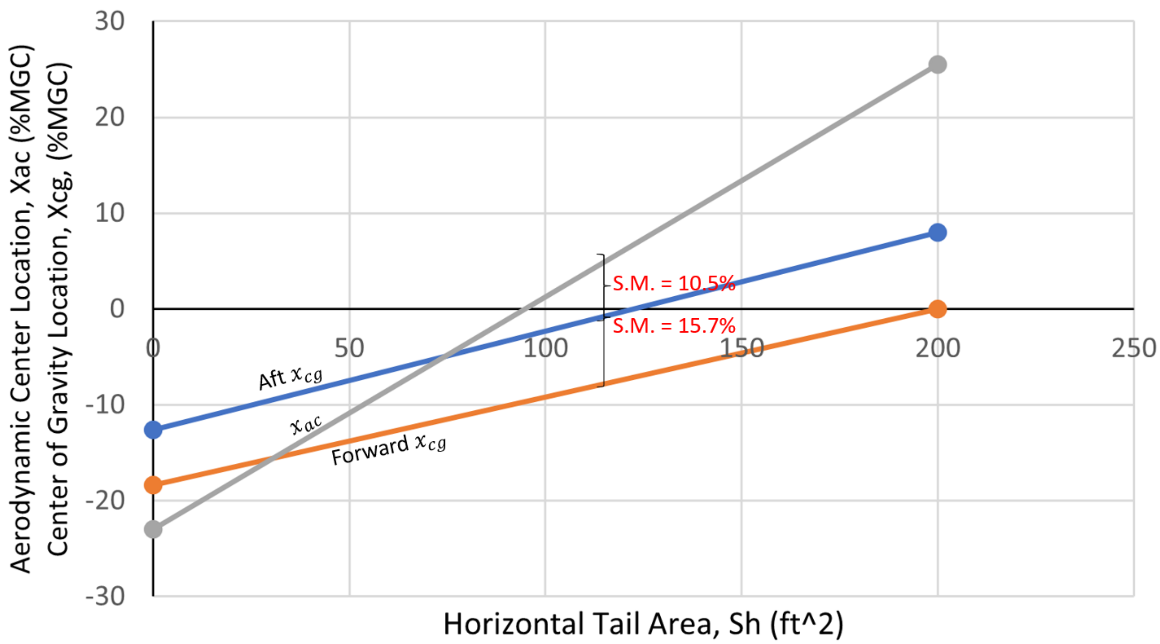

Figure 21.1: Longitudinal X-Plot

Directional analysis was then performed, calculating c_{n_β} as a function of vertical tail area. At the vertical tail area of 52.7 ft^2, c_{n_β} is calculated to be 0.00153 /degree. This is higher than the 0.001 /degree requirement, but additional directional stability is required for WIG operation so having a higher c_{n_β} value is desired. The directional x-plot can be seen in Figure 21.2 below.

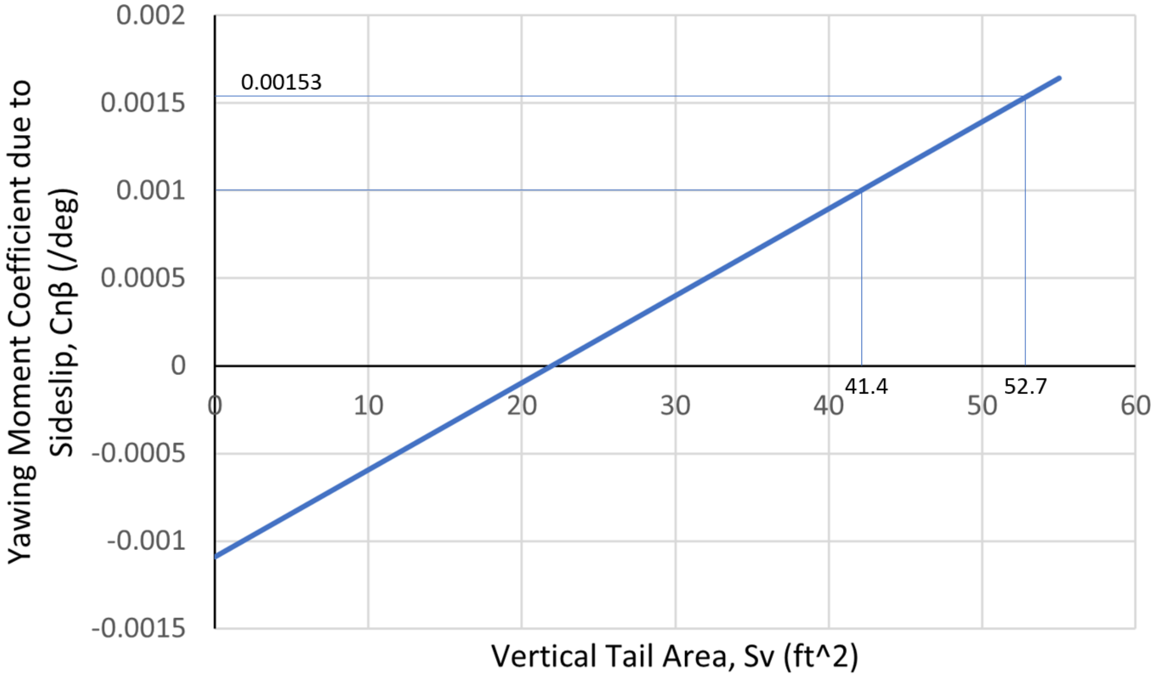

Figure 21.2: Directional X-Plot

22 Class II Stability and Control

In Class II stability and control analysis, various dynamic modes are considered. The requirements of these modes can be seen in this chapter. First the necessary ratios for dynamic longitudinal stability are given. The allowable short period damping ratios for dynamic longitudinal stability can be seen in Table 22.1 below.

Table 22.1: Allowable Short Period Damping Ratios for Dynamic Longitudinal Stability [28]

Handling Qualities	Category A and C Flight Phases	Category B Flight Phases
Level 1	$0.35<\zeta_{sp}<1.30$	$0.30<\zeta_{sp}<2.00$
Level 2	$0.25<\zeta_{sp}<2.00$	$0.20<\zeta_{sp}<2.00$
Level 3	$0.15<\zeta_{sp}$	$0.15<\zeta_{sp}$

The allowable phugoid damping ratios for dynamic longitudinal stability is given in Table 22.2.

Table 22.2: Allowable Phugoid Damping Ratios for Dynamic Longitudinal Stability [28]

Handling Qualities	Phugoid Stability Requirement
Level 1	$\zeta_{ph}>0.04$
Level 2	$\zeta_{ph}>0$
Level 3	$t_2>55$ sec

The necessary times to double amplitude for dynamic lateral-directional stability are then given. The time to double amplitude requirements for roll mode lateral-directional stability are given in Table 22.3 below.

Table 22.3: Time to Double Amplitude for Roll Mode Lateral-Directional Stability [28]

Flight Phase	Class	Level I	Level II	Level III
A	I, IV II, III	$t_R < 1.0$ sec. $t_R < 1.4$ sec.	$t_R < 1.4$ sec. $t_R < 3.0$ sec.	-
B	All	$t_R < 1.4$ sec.	$t_R < 3.0$ sec.	$t_R < 10$ sec.
C	I, II-C, IV II-L, C	$t_R < 1.0$ sec. $t_R < 1.4$ sec.	$t_R < 1.4$ sec. $t_R < 3.0$ sec.	-

The time to double amplitude requirements for spiral mode lateral-directional stability are then given in Table 22.4.

Table 22.4: Time to Double Amplitude for Spiral Mode Lateral-Directional Stability [28]

Flight Phase and Category	Level 1	Level 2	Level 3
A and C	$t_{2S} > 12$ sec.	$t_{2S} > 8$ sec.	$t_{2S} > 4$ sec.
B	$t_{2S} > 20$ sec.	$t_{2S} > 8$ sec.	$t_{2S} > 4$ sec.

The Frog Hopper is a class III aircraft and experiences category B and C flight. In addition to these specifications. The Frog Hopper will meet Level 1 flying qualities in all of the above listed categories.

23 Class II Systems

This section contains information pertaining to the many systems in the Frog Hopper aircraft.

23.1 Flight Control System

Irreversible flight controls are used on this aircraft utilizing electro hydrostatic actuators. Fiber optic signaling is also utilized in order to protect the flight controls in case of a lightning strike. There are inboard and outboard flaperons in the wing, as well as an elevator and rudder in the empennage. A schematic depicting the flight control system of the aircraft can be seen in Figure 23.1.1 below.

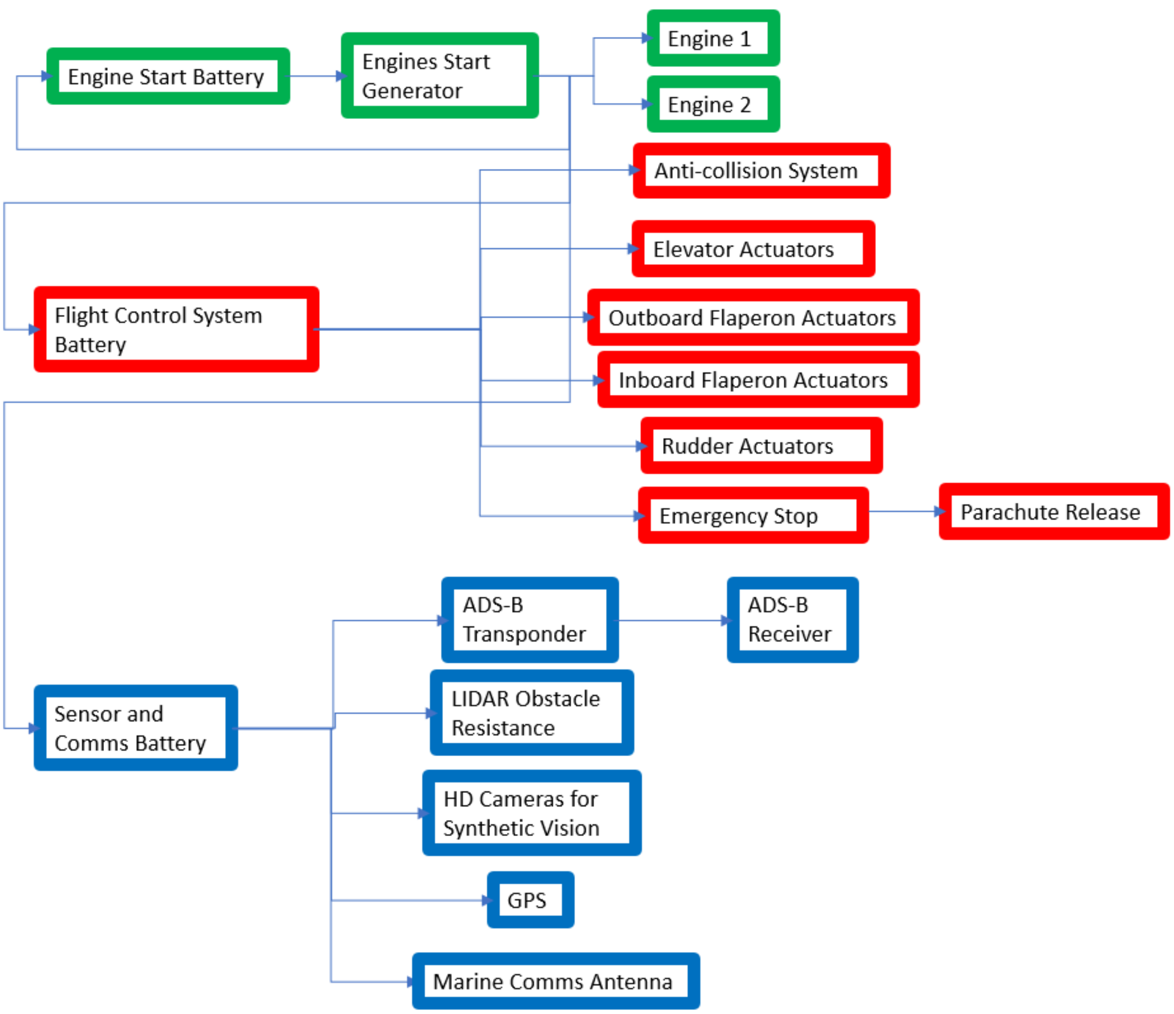

Figure 23.1.1: Flight Control System Schematic

The flight control lines are organized in a fashion such that they are triple-redundant. This is done to improve the flight safety of the aircraft, so if one or two of the flight control lines is damaged the aircraft can still land safely. The flight control lines are run along frames and longerons of the fuselage, as well as the forward and aft spars of the wing, horizontal tail, and vertical tail. The layout of the flight control system can be seen in Figure 23.1.2 below.

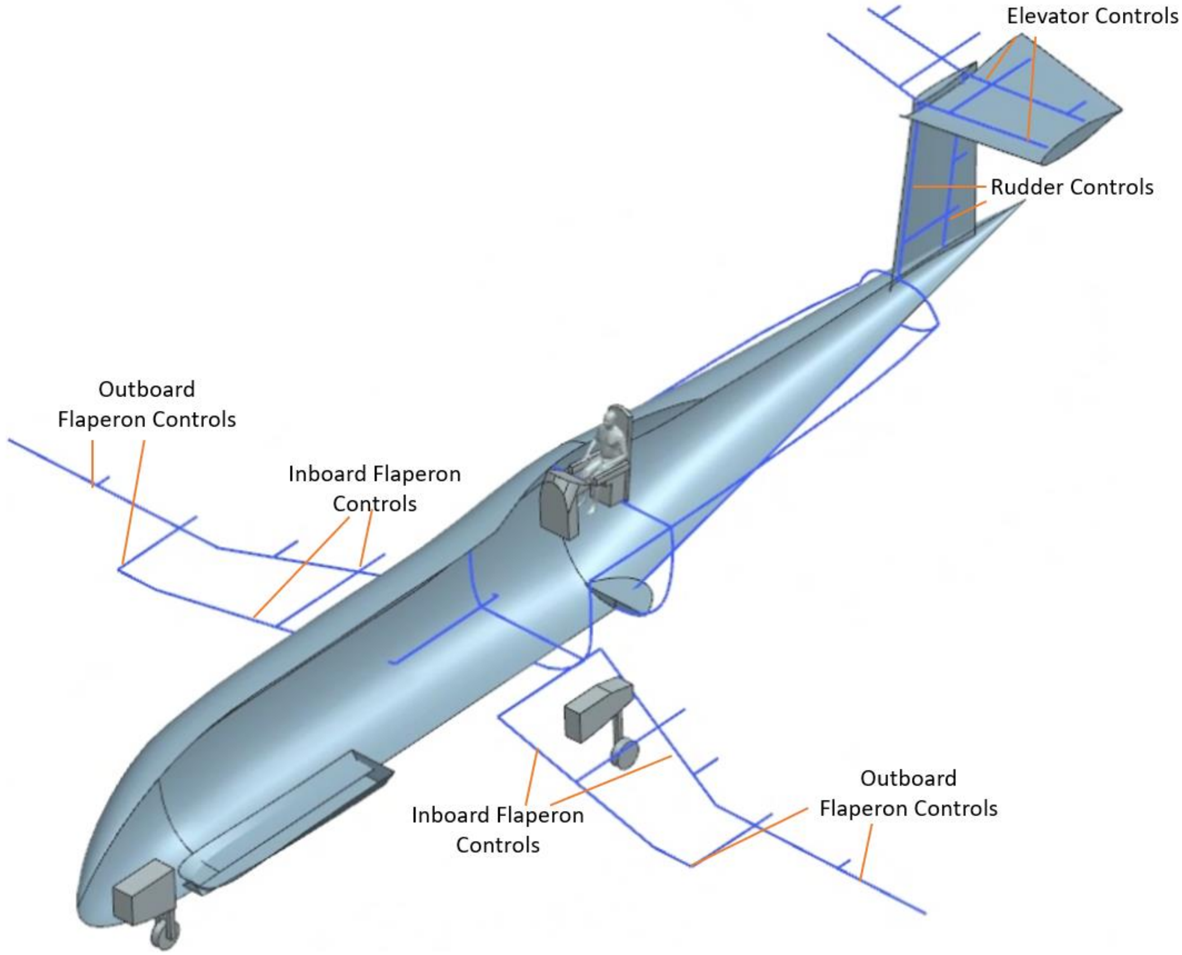

Figure 23.1.2: Flight Control System Layout

23.2 Fuel System

Due to the engines' locations compared to the wing's location, a pump feed system has to be used. The fuel weight at the maximum takeoff weight is 1565.5 pounds. In order to hold all of the required fuel, tanks in the wing hold 1165.5 pounds and tanks in the engine pylons hold 400 pounds. This distribution was chosen for center of gravity reasons. A refueling port was placed on the tail cone. This was done to allow for quick refueling while enplaning and deplaning. No fuel tanks were placed under or over the occupied cabin due to safety considerations. The fuel system can be seen in Figure 23.2.1 below.

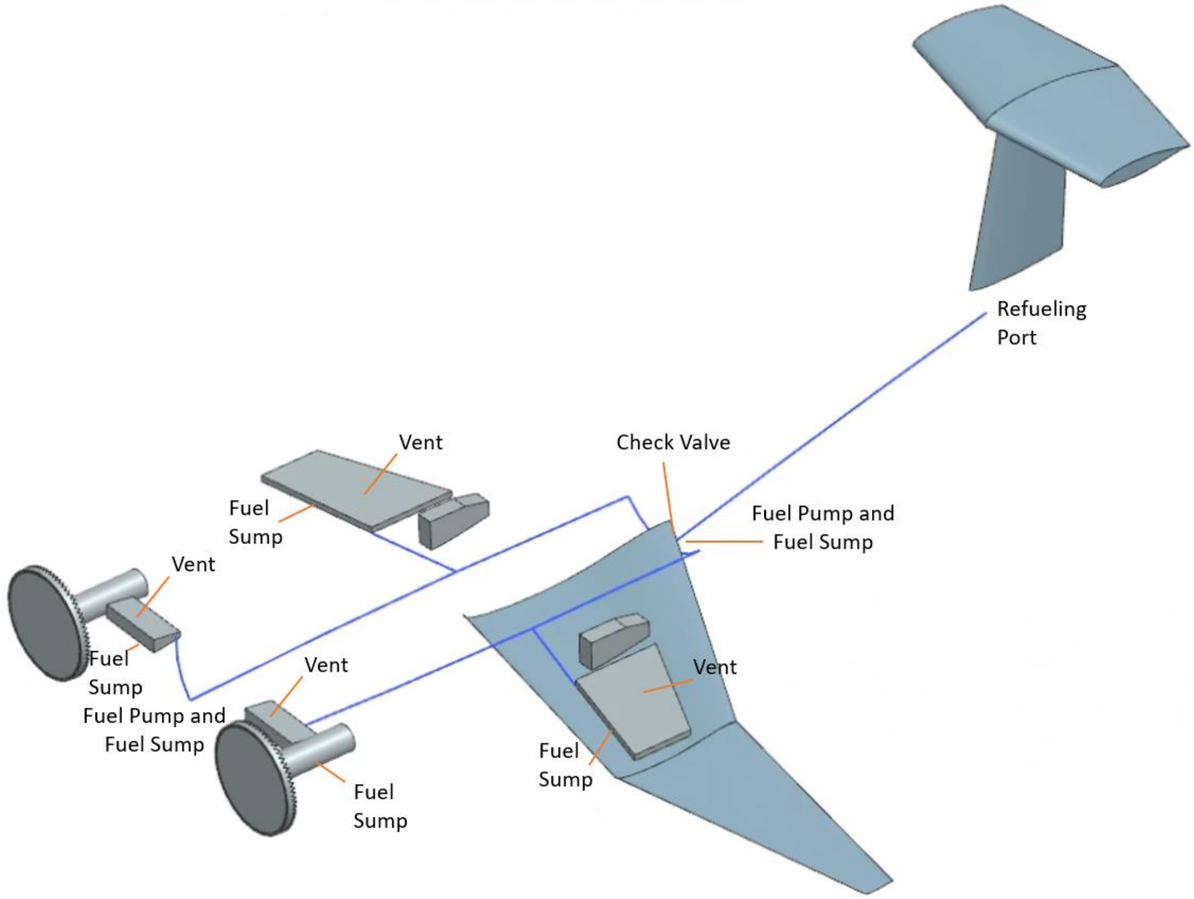

Figure 23.2.1: Fuel System Layout

Pumps are needed in areas where the fuel needs to travel upwards, against gravity. Sumps are also placed at the low points of the fuel tanks and the fuel system. This allows for drainage in the system. Vents are placed at the highest point of each fuel tank to allow for expansion and contraction at different altitudes. The landing gear bays were avoided when designing the fuel system, as landing gear could start a fire. Additionally, a check valve is placed where the left and right fuel lines meet. This is done to prevent the fuel CG from shifting off of the center line of the aircraft.

23.3 Hydraulic System

Hydraulics are no longer used for flight controls very often due to the limitations presented. Hydraulic systems still see use in landing gear deployment and brakes. The hydraulic system does not need to be triply redundant because the system is not flight critical. The hydraulic system layout can be seen in Figure 23.3.1 below.

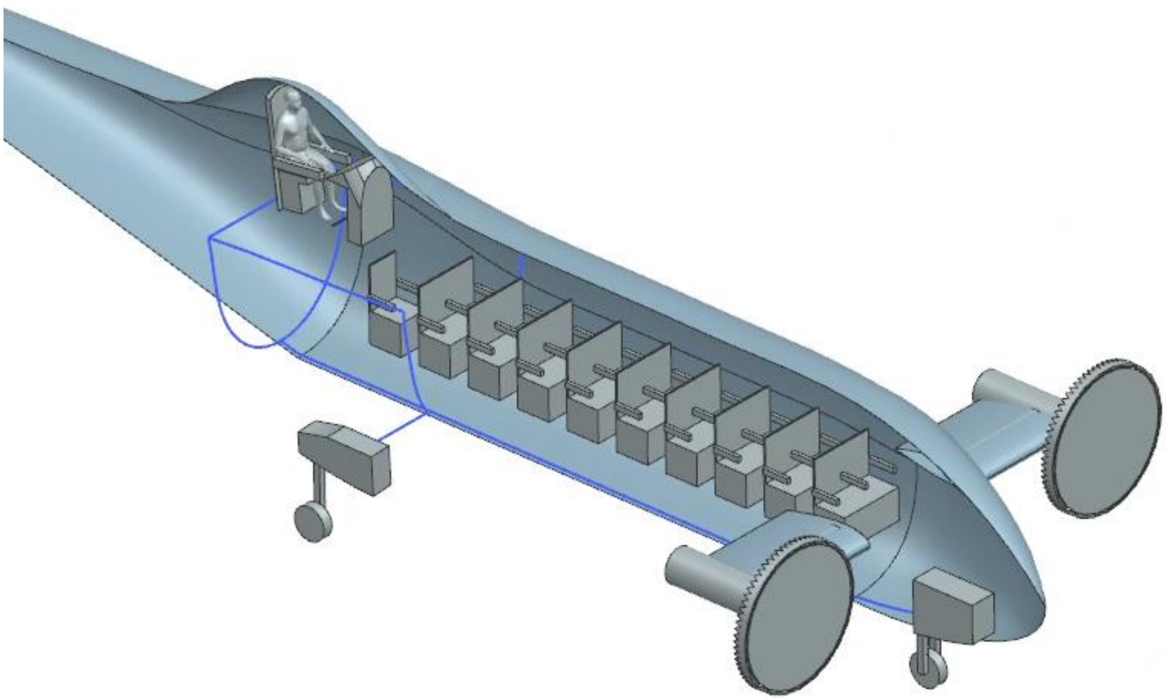

Figure 23.3.1: Hydraulic System Layout

The hydraulic system is run along the bottom longeron of the aircraft to the three landing gear of the aircraft.

23.4 Electrical System

The electrical system of the Frog Hopper aircraft contains many components. The avionics, fuel handling, and flight control systems are all critical components of the electrical system. There are also less critical systems in the lighting and air conditioning. An electrical system load summary was developed, and this can be seen below.

Table 23.4.1: Electrical Load Summary [28]

Load Summary	Power: Takeoff and Climb (V)	Power: Cruise (V)
Starter	28	0
Exterior Lighting	126	6.63
Flight Compartment Lighting	46.7	46.7
Passenger Cabin Lighting	463	480
Entertainment	0	98.0
Windshield Heating	196	235
Avionics	242	236
Air Conditioning	52.3	52.3
Fuel Handling	212	212
Hydraulics	287	0
Flight Control	65.3	65.3
Miscellaneous	8.16	8.16
Total	1726	1440

These electrical loads were calculated by scaling from a different passenger transport aircraft.

23.5 Environmental Control System

Due to this aircraft flying at a cruise altitude of 14,000 feet, it does not need to be pressurized. This means a pressurization system is not necessary in the aircraft. There is an air conditioning system for this aircraft. This is to allow for rapid cabin sterilization in the cabin. The air flow from the air conditioning system comes from the top of the fuselage, above each of the seats in the cabin. The air conditioning system will also increase passenger comfort throughout any flight.

23.6 Cockpit Instrumentation

Synthetic vision is necessary in the cockpit in order to allow for vision past the nose of the aircraft. This is due to the pod design of the cockpit. Additionally, light detection and ranging (LIDAR) detection is utilized to help avoid partially submerged obstacles while in its WIG configuration. Other instrumentation in the cockpit includes accelerometers, gyroscopes, fuel gages, speedometers, and altimeters. A very high frequency (VHF) radio is necessary to communicate with air traffic control during operation. For the Frog Hopper, the ARC-210 RT-2036 (C) Networked Communications Radio is specified [29]. This can be seen in Figure 23.6.1 below.

Figure 23.6.1: ARC-210 RT-2036 (C) Networked Communications Radio [29]

The option of satellite communications (SATCOM) will also be offered to potential customers of the Frog Hopper, via the HGA-2100B SATCOM High Gain Antenna and the HST-2110 High Speed Transceiver [30]. This option allows for on board wireless for the passengers of the aircraft.

23.7 Anti-Icing System

There are many different de-icing and anti-icing systems used in aircraft today. De-icer boots are older technology, but effective. These are comparably heavy to other systems and have been punctured in the past, however. Weeping wings are a popular chemical method of anti-icing used. Antifreeze is pumped through holes on the wing to keep ice from forming. The major downside of this method is that it works worse over time. This is because the holes get clogged with insects, dirt, and other debris. For the Frog Hopper, graphene resistance heaters will be used to prevent ice from forming. This is a relatively new anti-icing system, and research is continuing on it. The entry into service date for this aircraft is not until 2031, so it is feasible that these graphene resistance heaters have had more research supporting its usage then. One major advantage of this anti-icing system is its light weight. The lighter that systems such as anti-icing are, the better for the aircraft.

23.8 Window Rain, Fog, and Frost Control System

Wipers are often the system of choice for handling rain on the cockpit windshield. This is not feasible for the Frog Hopper however due to the pod design of the cockpit. Additionally, the cockpit windshield may be subject to more water due to this aircraft's amphibious nature and WIG configuration. Due to these factors, a hydrophobic coating will be applied to the cockpit windshield. This accommodates for the shape of the cockpit windshield as well as the amount of water it will face.

Frost control also needs to be considered for the cockpit. This will be achieved by having a conductive coating between the glass plies of the windshield. This was chosen due to the consistency that can be achieved by managing windshield frost using a conductive system.

24 Class I Structural Layout

Passenger visibility is an important aspect of this design, and thus influences ring frame spacing. A frame spacing of 30" was used as this matches the seat pitch in the cabin. This will allow for large windows for all passengers. These frames have a depth of 1.5". The longerons in the fuselage connect the ring frames together and carries load for the structure. Longerons are spaced more tightly together in the lower section of the fuselage, as

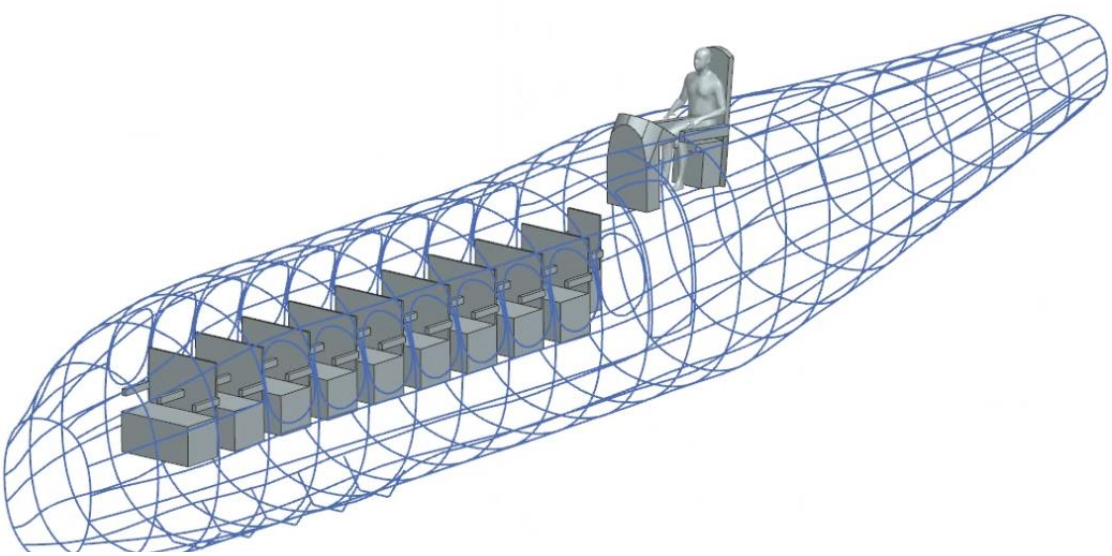

Figure 14.1: Class I Fuselage Structure

there is significant window space in the upper section of the fuselage. The majority of the longerons are spaced 15” apart, although they are spaced slightly tighter towards the bottom of the fuselage. Additionally, there is a frame around the cockpit pod, so that there isn’t load travelling through the glass. The cabin door and windows are placed in line with these ring frames and longerons. The structural layout of the fuselage can be seen below in Figure 14.1, along with the window and door frames of the aircraft.

To allow for maximum passenger visibility during flight, the cabin windows are designed to be a 28” wide and 34” tall oval. Increased passenger visibility will improve passenger satisfaction during the flight. The cabin door has the dimensions of 60” in height and 26” in width. The locations of the windows and door in comparison to the cabin seats can be seen in Figure 14.2 below.

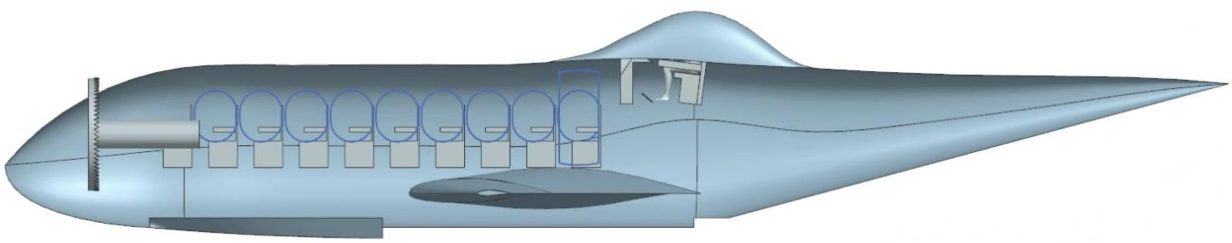

Figure 14.2: Window and Door Locations

The wing, horizontal tail, and vertical tail all have the front spar located at 20% of the chord while the aft spar is located at 70% of the chord. Ribs are then placed every 24” along the span of the planform.

25 Fault Tree Analysis

A fault tree analysis was performed to examine potential risks and failure points for the aircraft. The top-level main event that was considered for this analysis was catastrophic hull loss. This is a major failure that is necessary to avoid for the safety of all passengers. A fault tree analysis can be very expansive, so one branch of this full fault tree can be seen in Figure 15.1 below.

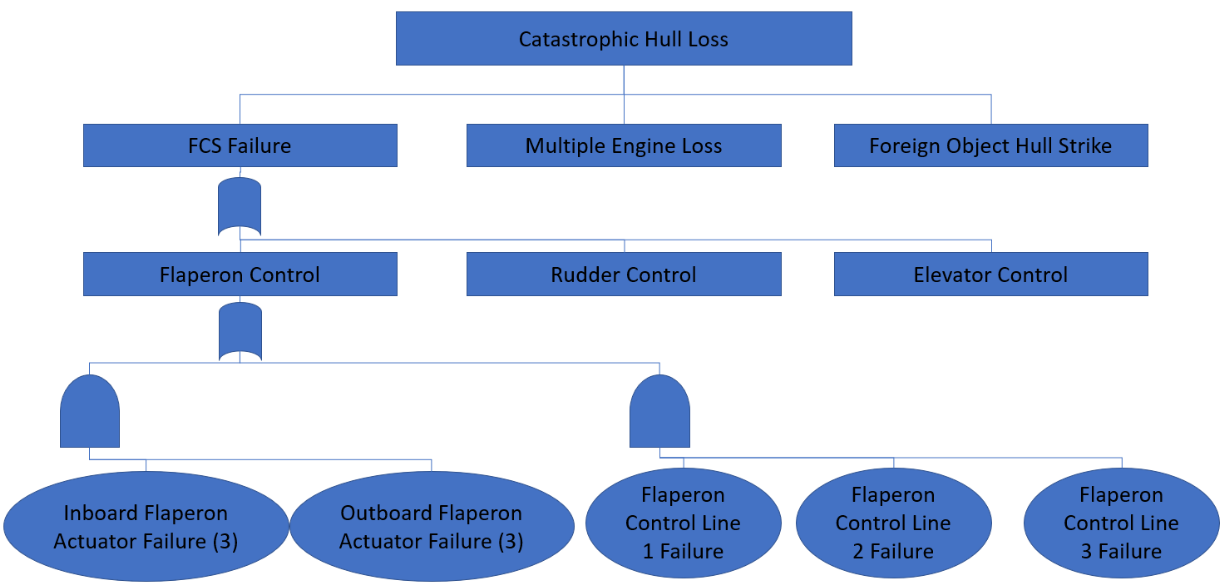

Figure 15.1: Catastrophic Hull Loss Fault Tree-Flaperon Branch

One of the events that can cause catastrophic hull loss is flight control system failure. The above image shows the specific events that would cause failure in the flaperon control. These events are actuator failure in both the inboard and outboard flaperons or the failure of all three flaperon control lines. The least reliable actuators fail at a rate of 1 in 10^2 events. This means that with three inboard flaperon actuators and three outboard flaperon actuators, the flaperon actuators would cause catastrophic hull loss at a significantly lesser rate than the 1 in 10^6 event rate that is required to satisfy FAR 23. By having the flight control system triply redundant, the chances of failure in the flight control lines causing hull loss are decreased significantly. Failure of the rudder control and failure of the elevator control are also caused by actuator failure and the failure of three flight control lines. The failure of any of these flight control surfaces could cause catastrophic hull loss in the aircraft and are therefore flight critical.

The loss of both engines is also a major cause of catastrophic hull loss. Bird strike is one of the main potential causes of the loss of both engines. To help mitigate this, cages are placed around the front of the engine. This will keep most birds from being ingested into the engine. In the case of larger birds compromising the engine, both engines would need to be breached to lead to catastrophic hull loss. Semi-submerged objects of significant size could also lead to a catastrophic breach of the hull. The structure of the hull is strengthened to accommodate for potential object strike, and closed cell foam is utilized to prevent the hull from taking on water. One major way that semi-submerged object strike can be mitigated is through the use of LIDAR detection. This allows for objects to be spotted by the pilot and avoided, preventing the hull being impacted at all.

26 Ground Operations

An important objective of the cargo mission is to achieve a turnaround time under 60 minutes. In order to examine the feasibility of this, the turnaround time of a larger aircraft, the CRJ100, is examined. The breakdown of the turnaround of the CRJ100 was obtained from the airport planning manual for the aircraft and can be seen in Figure 26.1 below.

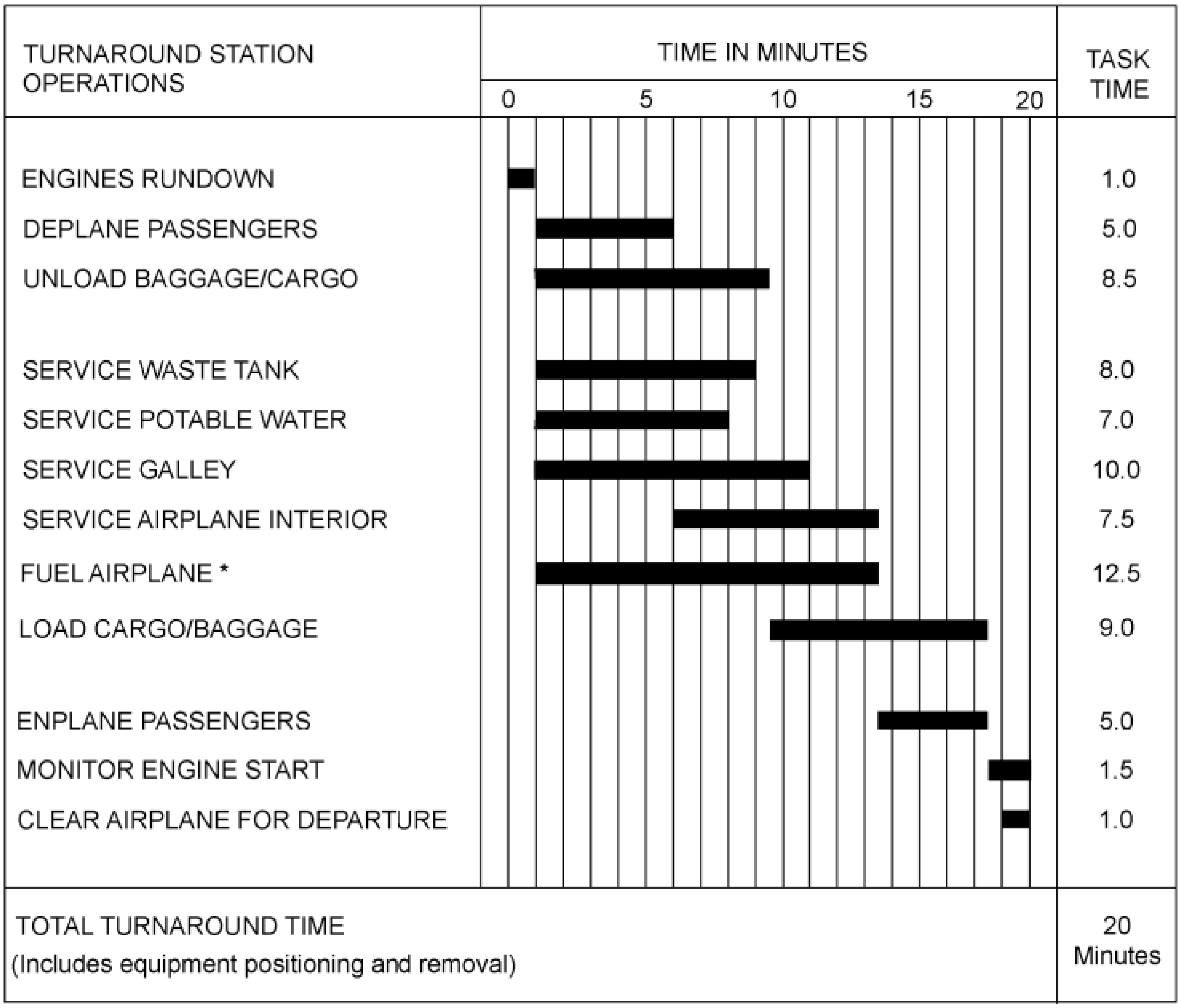

Figure 26.1: CRJ100 Turnaround Time Breakdown [31]

The CRJ100 is a 50-seat aircraft, and the Frog Hopper does not have a galley or lavatory that needs to be serviced, further decreasing the turnaround time. Based on this information, a turnaround time of 20 minutes is achievable for the Frog Hopper aircraft. This achieves both the requirement set forth in the RFP as well as the objective set forth by the author. The location of the fuel port on the tail cone will allow for fueling to occur out of the way of other turnaround tasks such as cargo reloading.

The passenger baggage volume requirement of 4 $\frac{ft^3}{pax}$ is also verified to be met. This results in a total baggage volume of 76 ft^3. The baggage hold for the Frog Hopper is below the cabin of the aircraft. Due to the aircraft's operation off of water, the lowest that baggage is held is a foot off of the floor of the aircraft fuselage. This is because hull structure allowing for potential semi-submerge obstacle strikes and closed cell foam takes up this first layer. This is done to keep any gash in the hull of the aircraft from ruining the luggage of passengers. The volume of the baggage hold was found using Siemens NX. This can be seen in Figure 26.2 below.

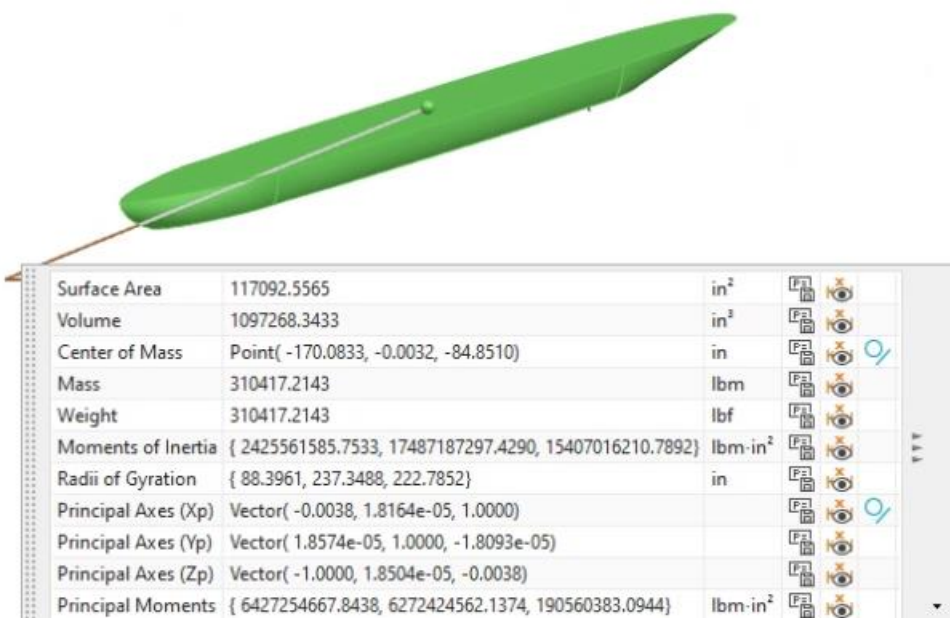

Surface Area	117092.5565	in²
Volume	1097268.3433	in³
Center of Mass	Point(-170.0833, -0.0032, -84.8510)	in
Mass	310417.2143	lbm
Weight	310417.2143	lbf
Moments of Inertia	{ 2425561585.7533, 17487187297.4290, 15407016210.7892}	lbm·in²
Radii of Gyration	{ 88.3961, 237.3488, 222.7852}	in
Principal Axes (Xp)	Vector(-0.0038, 1.8164e-05, 1.0000)	
Principal Axes (Yp)	Vector(1.8574e-05, 1.0000, -1.8093e-05)	
Principal Axes (Zp)	Vector(-1.0000, 1.8504e-05, -0.0038)	
Principal Moments	{ 6427254667.8438, 6272424562.1374, 190560383.0944}	lbm·in²

Figure 26.2: Baggage Hold Volume Verification

As demonstrated in the above image, the volume is calculated to be 1,097,268 in^3. This is equivalent to 635 ft^3, which more than satisfies the total baggage requirement. This also allows for passengers' baggage to vary greatly in shape. This meets the passenger baggage volume requirement given in the RFP.

Passenger boarding and deplaning is an important consideration. The cabin door is on top of the wing, meaning passengers will have to enter and exit the plane over the wing. Due to this, textured strips 18 inches thick are placed from the door to the leading edge of the wing. This allows passengers to safely walk on this section of the wing when boarding and deplaning. From the leading edge, ramps are used to reach the ground or dock, depending on the place where the aircraft is taking off or landing from. For flights off of land, a ramp extends from the leading edge at a 15° decline. This ramp changes directions so that it avoids the Frog Hopper's engines. The ramp for boarding and deplaning passengers on land can be seen in Figure 26.3 and Figure 26.4 below.

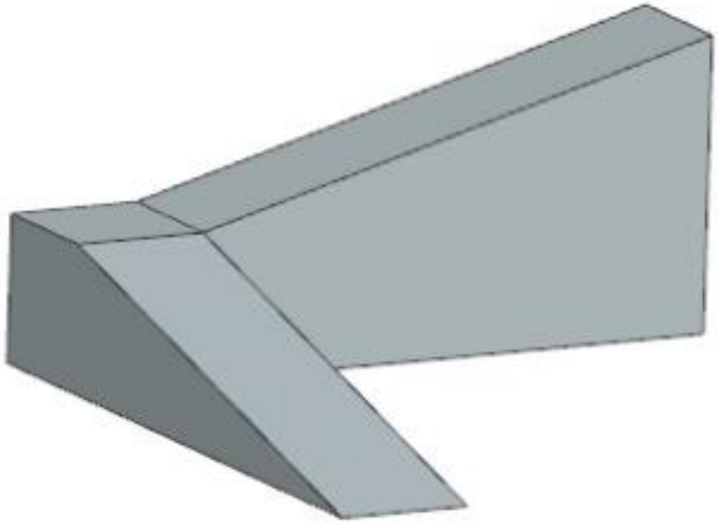

Figure 26.3: Passenger Land Ramp

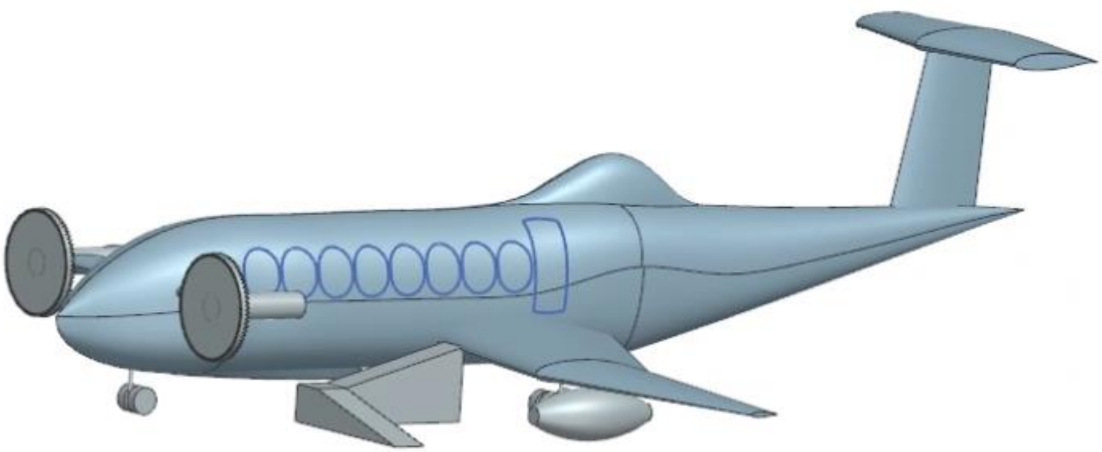

Figure 26.3: Passenger Land Ramp with Aircraft

The boarding and deplaning ramp for water takeoff and landing is flat from the leading edge of the wing along the span. This allows for passengers to walk directly to the dock without stepping foot in the water. This is done to satisfy the dry disembarkation at dock objective set forth by the author. The ramp for water takeoffs and landing can be seen in Figure 26.4 and Figure 26.5 below.

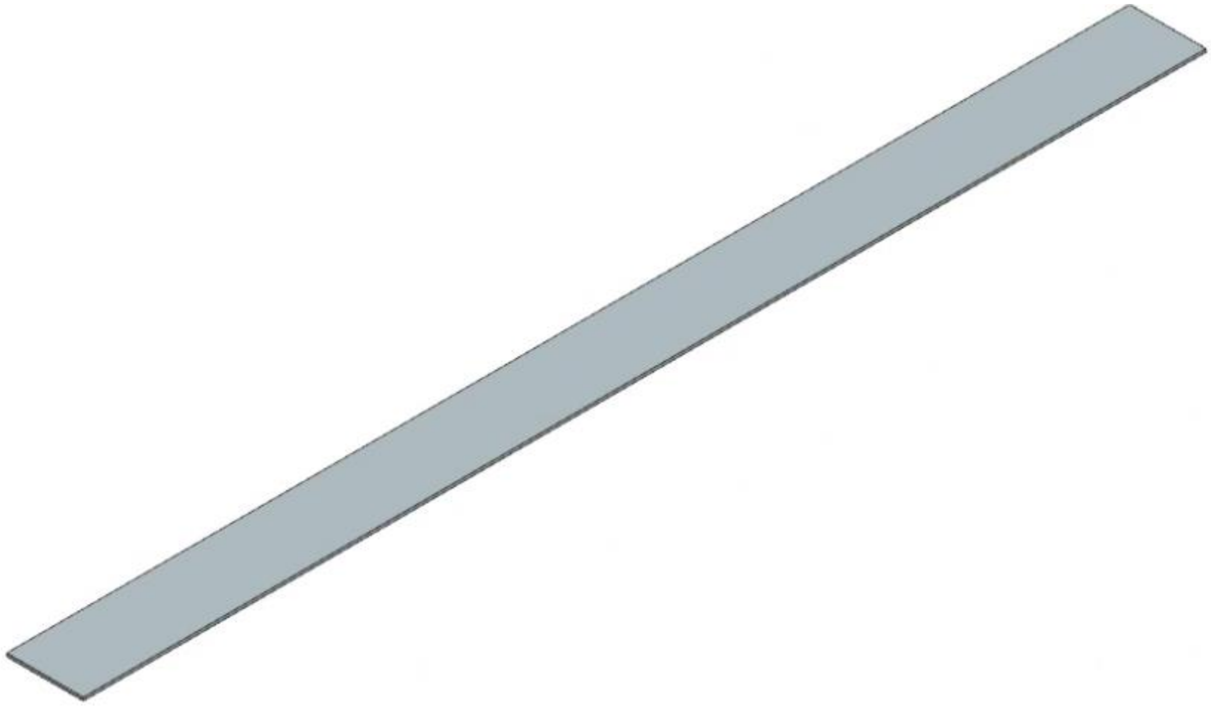

Figure 26.4: Passenger Water Ramp

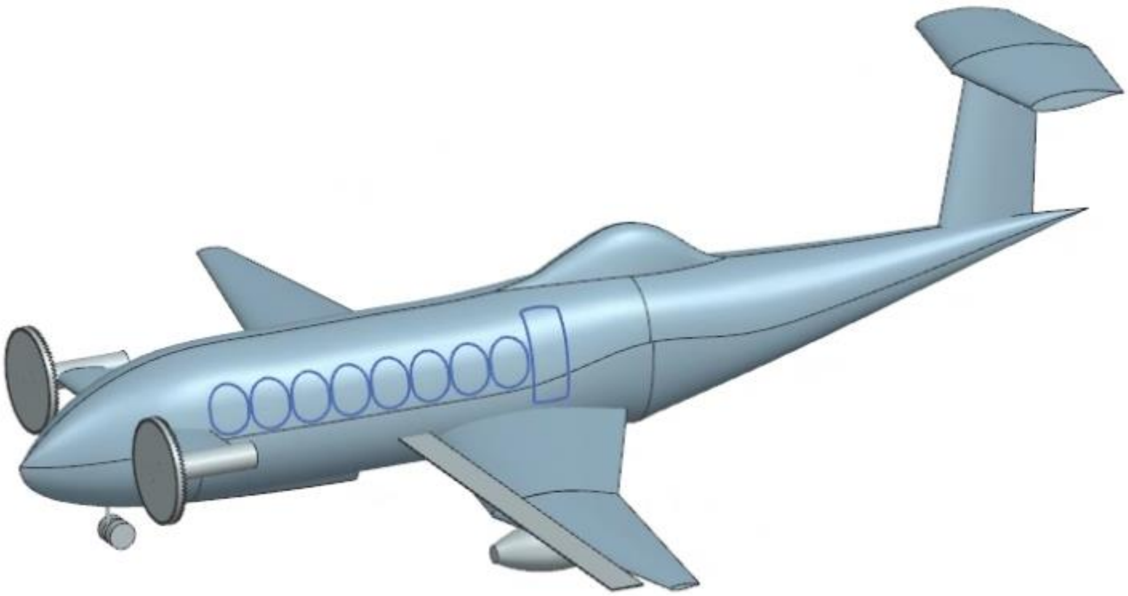

Figure 26.5: Passenger Water Ramp with Aircraft

The reason ramps are used rather than a staircase is to maintain ADA compliance. This will allow for easier boarding and deplaning for wheelchair users.

27 Performance

In order to verify the performance of the Frog Hopper aircraft, the range must be calculated. The passenger mission has a range requirement of 250 nmi, so the amount of fuel must satisfy this range. The fuel load was calculated to be 1566 lb during Class I weight sizing. This was used with the Breguet Range equation: $R(nmi) = 325.9\left(\frac{nmi-lbf}{hp-hr}\right) * \left\{\frac{\eta_p}{c_p\left(\frac{lbf}{hp-hr}\right)}\right\} * \left(\frac{L}{D}\right) \ln\left(\frac{W_i}{W_f}\right)$. The relevant values of the equation can be seen in Table 16.1 below.

Table 27.1: Breguet Range Equation Values

Characteristic	Value
η_p	0.9
c_p	$0.54\,\frac{lbf}{hp-hr}$
$\frac{L}{D}$	8.84
W_i	15500 lb
W_f	$15500 - 1566 = 13934\ lb$

This results in a range of 511 nmi. This satisfies the range requirement for the passenger mission, as well as the two other specified missions.

28 Cost Analysis

The cost of developing and manufacturing a run of the Frog Hopper was estimated. The research, development, technology, and engineering (RDT&E) costs were calculated first. For the development phase, four aircraft are built. The components of the RDT&E costs are broken down in Table 28.1 below.

Table 28.1: RDT&E Cost Breakdown

Cost	Value
Airframe Engineering and Design Cost	$68,867,932
Development Support and Testing Cost	$15,072,443
Flight Test Aircraft Cost	$290,624,564
Engines and Avionics Cost	$4,574,130
Manufacturing Labor Cost	$131,032,346
Materials Cost	$20,400,910
Tooling Cost	$117,582,973
Quality Control Cost	$17,034,205
Flight Test Operations Cost	$703,096
Profit	$27,458,636
Financing Cost	$54,917,273
Total RDT&E Cost	$457,643,945

The materials cost for the aircraft is based on PEEK/graphite composite. This strong, lightweight composite material is used for the majority of the primary structure of the aircraft. A production run of 1,000 aircraft was then decided upon for the Frog Hopper. This was decided upon because this aircraft serves a very similar market to the De Havilland Canada DHC-6 Twin Otter, which had 832 units. In addition to this market, the Frog Hopper also serves commutes in coastal cities and tourism related flights in the WIG configuration. This led to the production run increasing to 1,000 aircraft. The cost breakdown for the production run can be seen in Table 28.2 below.

Table 28.2: Production Run Cost Breakdown

Cost	Value
Airframe Engineering and Design Cost	$120,434,997
Aircraft Program Production Cost	$6,693,469,254
Engines and Avionics Cost	$2,287,065,000
Interiors Cost	$45,030,000
Manufacturing Labor Cost	$2,239,291,490
Materials Cost	$1,602,123,077
Tooling Cost	$228,851,793
Quality Control Cost	$291,107,894
Production Flight Test Operations Cost	$4,382,000
Profit	$1,203,226,985
Financing Cost	$1,203,226,985
Total Production Cost	$9,224,740,221

29 Situational Renderings

Situational renderings were made for both the Frog Hopper-100FF configuration and the Frog Hopper-100W configuration. These can be seen in Figure 29.1, Figure 29.2, Figure 29.3, and Figure 29.4 below.

Figure 29.1: Frog Hopper-100FF Parked

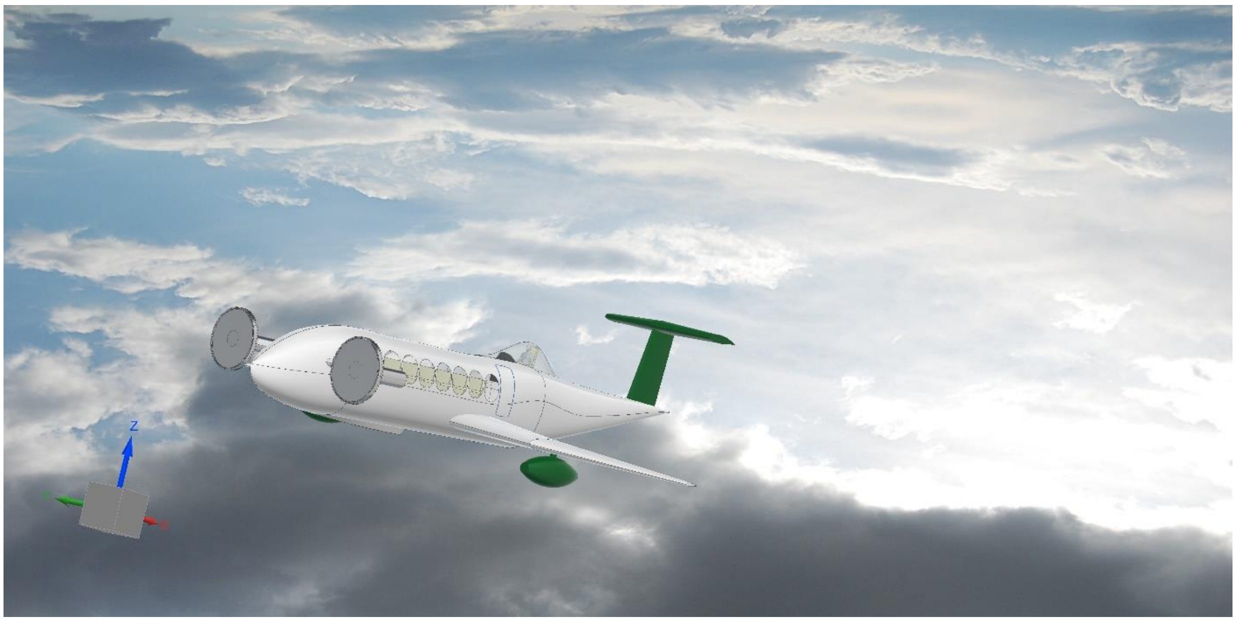

Figure 29.2: Frog Hopper-100FF In Flight

Figure 29.3: Frog Hopper-100W Docked

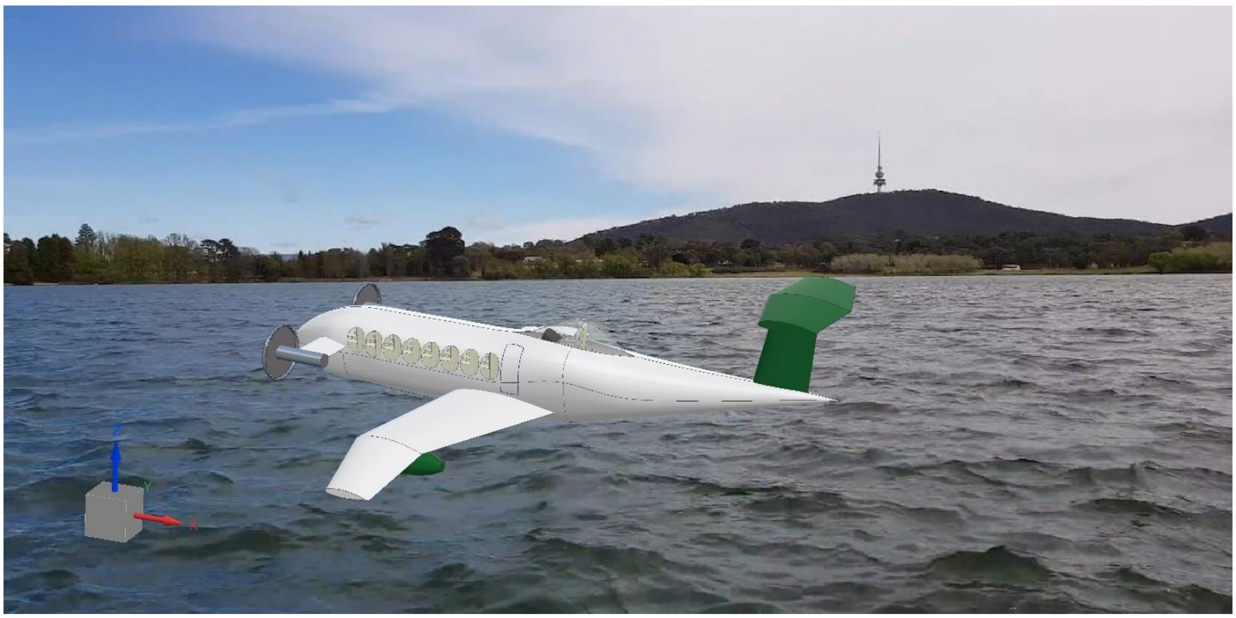

Figure 29.4: Frog Hopper-100W In Flight

30 References

1. "New Efficient Water and Terrestrial (NEWT) Aircraft," Aircraft Design Technical Committee, AIAA, 2022
2. Schwartzhoff, Riley, "Homework 4," University of Kansas, 1 Nov. 2022
3. Schwartzhoff, Riley, "Homework 5," University of Kansas, 1 Nov. 2022
4. "Jane's All The World's Aircraft: In Service," Jane's Group UK, 2022
5. "Beechcraft 1900," Wikipedia, https://en.wikipedia.org/wiki/Beechcraft_1900#:~:text=The%20Beechcraft%201900%20is%20a,several%20governmental%20and%20military%20organizations., Accessed 12:00 PM, 29 Jan, 2023.
6. "British Aerospace Jetstream," Wikipedia, https://en.wikipedia.org/wiki/British_Aerospace_Jetstream, Accessed 12:00 PM, 29 Jan, 2023.
7. "De Havilland Canada DHC-6," Wikipedia, https://en.wikipedia.org/wiki/De_Havilland_Canada_DHC-6_Twin_Otter, Accessed 12:00 PM, 29 Jan, 2023.
8. "Jane's All The World's Aircraft: Development & Production," Jane's Group UK, 2022
9. "Dornier 228," Wikipedia, https://en.wikipedia.org/wiki/Dornier_228#Operators, Accessed 12:00 PM, 29 Jan, 2023.
10. "Harbin Y-12," Wikipedia, https://en.wikipedia.org/wiki/Harbin_Y-12, Accessed 12:00 PM, 5 Feb, 2023.
11. "Britten-Norman Trislander," Wikipedia, https://en.wikipedia.org/wiki/Britten-Norman_Trislander, Accessed 12:00 PM, 5 Feb, 2023.
12. "Cessna 408 SkyCourier," Wikipedia, https://en.wikipedia.org/wiki/Cessna_408_SkyCourier, Accessed 12:00 PM, 5 Feb, 2023.
13. "PZL M28 Skytruck," Wikipedia, https://en.wikipedia.org/wiki/PZL_M28_Skytruck, Accessed 12:00 PM, 5 Feb, 2023.
14. "Dornier Seastar," Wikipedia, https://en.wikipedia.org/wiki/Dornier_Seastar, Accessed 12:00 PM, 5 Feb, 2023.
15. "Canadair CL-415," Wikipedia, https://en.wikipedia.org/wiki/Canadair_CL-415, Accessed 12:00 PM, 5 Feb, 2023.

16. “Beechcraft 1900,” OneSpotter, https://onespotter.com/type/890/1900%20Airliner, Accessed 12:00 PM, 5 Feb, 2023.
17. “British Aerospace Jetstream 31,” AirlineFleet, http://www.airlinefleet.info/images/prodlist/baej31/zzb-baej31.pdf, Accessed 12:00 PM, 5 Feb, 2023.
18. “Dornier 228,” OneSpotter, https://onespotter.com/type/972/Do%20228, Accessed 12:00 PM, 5 Feb, 2023.
19. “De Havilland Canada DHC-6,” AirlineFleet, http://www.airlinefleet.info/images/prodlist/dhc6/zzb-dhc6.pdf, Accessed 12:00 PM, 5 Feb, 2023.
20. Atanasov, G., van Wensveen, J., Peter, F., and Zill, T., “Electric Commuter Transport Concept Enabled by Combustion Engine Range Extender,” DLRK 2019, 30 Sep. 2019.
21. “Dornier Seawings Seastar,” http://www.flugzeuginfo.net/acdata_php/acdata_cd2_en.php, Accessed 1:30 PM, 12 Feb, 2023.
22. “Canadair/Bombardier CL-415/Bombardier 415,” http://www.flugzeuginfo.net/acdata_php/acdata_cl415_en.php, Accessed 1:30 PM, 12 Feb, 2023.
23. “Pratt and Whitney Canada PT6,” Wikipedia, https://en.wikipedia.org/wiki/Pratt_%26_Whitney_Canada_PT6#Specifications_(PT6A-6), Accessed 8:00 PM, 19 Feb. 2023.
24. “Civil Turboshaft/Turboprop Specifications,” https://jet-engine.net/civtsspec.htm, Accessed 8:00 PM, 19 Feb. 2023.
25. Bodlak, E., Chawla, D., Jaju, V., Kolli, J.T., Patil, A., and Schumacher, L., “AE 722 Design Report Number 6: The BATWinG Air Taxi,” University of Kansas, 13 Apr. 2015.
26. Roskam, J., “Airplane Design Part IV: Layout of Landing Gear and Systems,” DARcorporation, 1985.
27. Roskam, J., “Airplane Design Part V: Component Weight Estimation,” DARcorporation, 1985.
28. Roskam, J., “Airplane Design Part VII: Determination of Stability, Control, and Performance Characteristics: FAR and Military Requirements,” DARcorporation, 1985.

29. "Airborne VHF/UHF/L-Band," Collins Aerospace, https://www.collinsaerospace.com/what-we-do/industries/military-and-defense/communications/airborne-communications/satcom, Accessed 3:30 PM, 8 May, 2023.
30. "Airborne SATCOM," Collins Aerospace, https://www.collinsaerospace.com/what-we-do/industries/military-and-defense/communications/airborne-communications/satcom, Accessed 3:30 PM, 8 May, 2023.
31. "Canadair Regional Jet Model CL-600-2B19 Series 100/200/440 Airport Planning Manual," Bombardier Inc, 10 Jan, 2016